Environmental Science & Technology

Critical Review

pubs.acs.org/est

New Constraints on Terrestrial Surface−Atmosphere Fluxes of Gaseous Elemental Mercury Using a Global Database

Yannick Agnan,*[,†] Théo Le Dantec,[‡,§] Christopher W. Moore,[†] Grant C. Edwards,[∥] and Daniel Obrist*[,†]

[†]Division of Atmospheric Sciences, Desert Research Institute, Reno, Nevada 89523, United States

[‡]Université de Toulouse; INP, UPS; EcoLab (Laboratoire Ecologie Fonctionnelle et Environnement); ENSAT, Avenue de l'Agrobiopole, F-31326 Castanet-Tolosan, France

[§]CNRS; EcoLab; F-31326 Castanet-Tolosan, France

[∥]Department of Environmental Sciences, Faculty of Science and Engineering, Macquarie University, Sydney, New South Wales, Australia

Supporting Information

ABSTRACT: Despite 30 years of study, gaseous elemental mercury (Hg^0) exchange magnitude and controls between terrestrial surfaces and the atmosphere still remain uncertain. We compiled data from 132 studies, including 1290 reported fluxes from more than 200 000 individual measurements, into a database to statistically examine flux magnitudes and controls. We found that fluxes were unevenly distributed, both spatially and temporally, with strong biases toward Hg-enriched sites, daytime and summertime measurements. Fluxes at Hg-enriched sites were positively correlated with substrate concentrations, but this was absent at background sites. Median fluxes over litter- and snow-covered soils were lower than over bare soils, and chamber measurements showed higher emission compared to micrometeorological measurements. Due to low spatial extent, estimated emissions from Hg-enriched areas (217 $Mg{\cdot}a^{-1}$) were lower than previous estimates. Globally, areas with enhanced atmospheric Hg^0 levels (particularly East Asia) showed an emerging importance of Hg^0 emissions accounting for half of the total global emissions estimated at 607 $Mg{\cdot}a^{-1}$, although with a large uncertainty range (−513 to 1353 $Mg{\cdot}a^{-1}$ [range of 37.5th and 62.5th percentiles]). The largest uncertainties in Hg^0 fluxes stem from forests (−513 to 1353 $Mg{\cdot}a^{-1}$ [range of 37.5th and 62.5th percentiles]), largely driven by a shortage of whole-ecosystem fluxes and uncertain contributions of leaf-atmosphere exchanges, questioning to what degree ecosystems are net sinks or sources of atmospheric Hg^0.

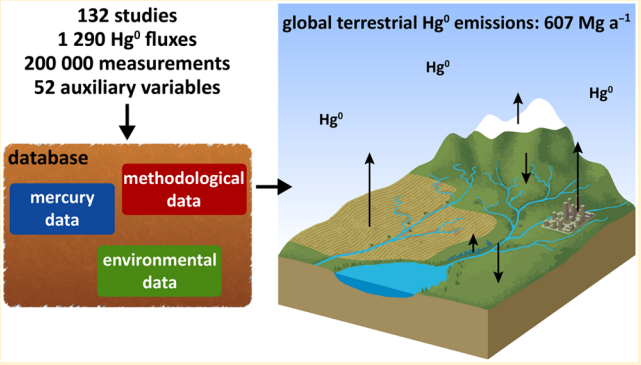

1. INTRODUCTION

Gaseous elemental mercury (Hg^0) is the dominant form of mercury (Hg) in the atmosphere[1,2] with background levels generally from 1.0 to 1.7 ng m^{-3} in the Northern Hemisphere[3−5] and from 0.5 to 1.2 ng m^{-3} in the Southern Hemisphere.[6−9] Between 29 and 33% of all atmospheric emissions stem from primary anthropogenic sources (artisanal and industrial mining, coal and fuel combustion, waste treatment, chloro-alkali production, and others), and between 5 and 13% from primary natural geogenic sources (e.g., volcanism and soil/rock alteration).[10−15] Secondary emissions—Hg^0 re-emissions of previous deposition, also called legacy emissions—are considered an important flux in the global Hg biogeochemical cycle, accounting for an estimated 56−65% of total atmospheric Hg emissions.[15−17] A key significance of such re-emissions is that they ultimately expand both the spatial and temporal extent of Hg pollution via multiple surface−atmosphere exchanges (or hopping) and the underlying reason for re-emissions is that Hg^0 has a high vapor pressure (163×10^{-3} Pa at 20 °C), is semivolatile, and is readily exchanged between surfaces (e.g., vegetation, soils, snow, ice, and water) and the atmosphere (i.e., deposition and emission).[18−21]

Hg^0 surface−atmosphere exchange has been extensively studied in Hg-enriched sites (both naturally enriched and atmospherically influenced)[22−26] and background sites[27−30] during the last 30 years. By scaling up field measurements from 46 sites across the United States, Ericksen et al.[31] estimated annual natural Hg^0 emissions of 52 $Mg{\cdot}a^{-1}$ from Hg-enriched soils and net emission of 43 $Mg{\cdot}a^{-1}$ from background soils in the United States. These calculations suggest that background areas also contribute significantly to atmospheric Hg^0 emissions

Received: August 20, 2015
Revised: November 23, 2015
Accepted: November 24, 2015
Published: November 24, 2015

DOI: 10.1021/acs.est.5b04013
Environ. Sci. Technol. 2016, 50, 507−524

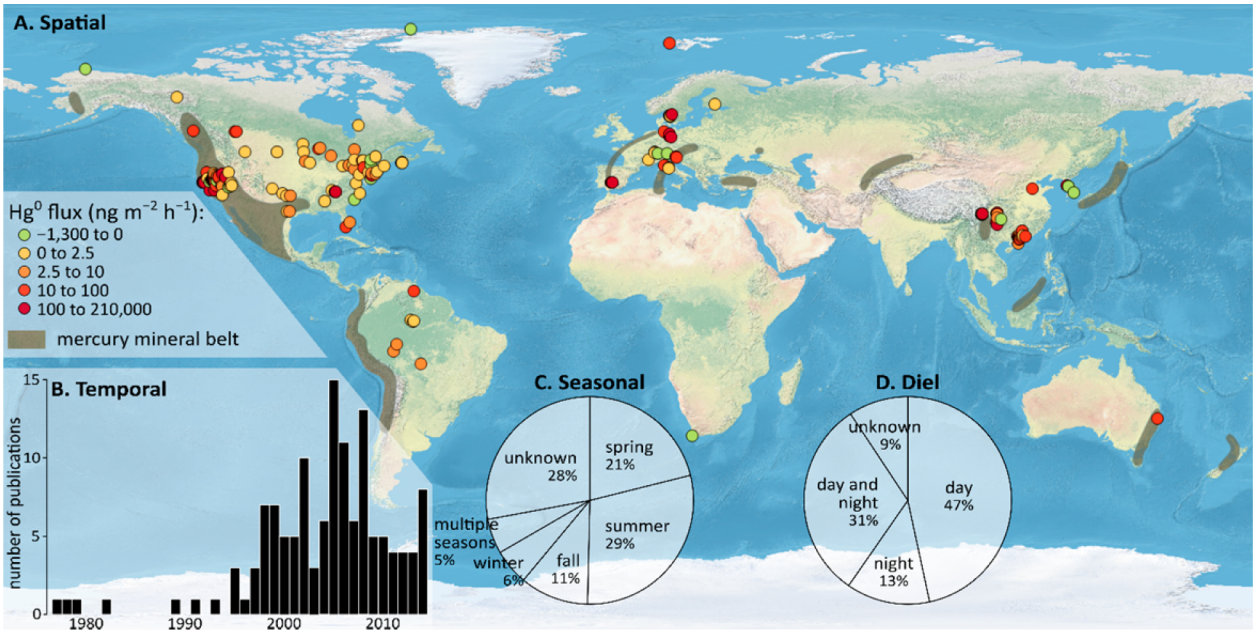

Figure 1. Coverage of study sites by averaged Hg^0 flux (the brown areas correspond to the terrestrial mercury mineral belts,[58,59] **A**), number of publications per year along with (**B**), seasonal (**C**) and diel (**D**) proportions of measurements.

despite low soil Hg concentrations and therefore low atmospheric emission potential.[32,33]

Hg^0 flux studies thus far have revealed several important environmental factors that modulate Hg^0 fluxes from terrestrial surfaces, including the following: (1) solar radiation[26,34−36] which induces photoreduction;[37] (2) air and soil temperatures with higher temperatures generally stimulating Hg^0 evasion;[22,38,39] (3) precipitation and soil moisture that stimulate emissions at some sites but reduce emissions at others;[22,25,29,40−44] and (4) atmospheric Hg^0 concentrations that also have both positive and negative effects on fluxes.[18,26,45,46] Effects of these variables have been quantified in many studies, while other potentially important controls have been poorly characterized—including, for example, the roles of UV−B radiation,[47,48] litter cover,[49,50] or overburden at geogenic sites.[48,51] The importance of all factors, however, appears to vary from site to site and study to study.[52,53]

We performed a comprehensive comparison of previous study results with the intent to constrain uncertainties such as the large range in magnitude of reported Hg^0 fluxes and discrepancies in the processes that control Hg^0 exchange among sites and studies, and ultimately to better quantify the magnitude of terrestrial-atmosphere fluxes. To complete this analysis, we created a new global database integrating terrestrial Hg^0 flux measurements and controlling processes available in the literature. Further, we aimed to (1) characterize the spatial and temporal coverage of current global terrestrial surface−atmosphere Hg^0 measurements; (2) evaluate the magnitude of Hg^0 fluxes over terrestrial surfaces with different levels of Hg contamination and by various land cover types; (3) compare influences of environmental variables that control Hg^0 fluxes and their consistency across studies and across the global data set; (4) determine if the measurement method causes differences in Hg^0 fluxes; and finally (5) constrain net global-scale terrestrial Hg^0 exchange using statistical frequency distribution and confidence intervals for various ecosystems and soil Hg burdens.

2. GLOBAL HG^0 FLUX DATABASE

The structure of the Hg^0 flux database was developed to integrate a large amount of published data including environmental and methodological information and on factors controlling Hg^0 exchange across a variety of different terrestrial ecosystems and surfaces (Figure S1, Supporting Information). This database included factors well-known in the literature to influence Hg^0 exchange, such as substrate Hg concentration; air temperature; measurement methodology; as well as environmental variables, such as land cover, surface type, and soil cover (e.g., litter or snow). We compiled a comprehensive set of 52 auxiliary variables for evaluation and synthesis of Hg^0 fluxes in the data set, although not all variables were available for each study. Each data entry corresponds to one Hg^0 flux reported in a study−consisting of subhourly, hourly, daily, monthly, or annual flux measurement averages.

Based on the number of individual flux measurements reported from the 132 scientific studies included in the database, we estimated that the data set represented more than 200 000 individual flux measurements. Since raw data of individual flux measurements were generally unavailable to extract from published papers, we worked with partially averaged and summarized (i.e., aggregated) data. This also had the advantage that outliers, unusually high variability, or unreasonable flux data already had been removed by the individual author's quality control and assurance protocols during publication of the respective studies. The database, therefore, contained 1290 Hg^0 flux measurements. Although these measurements represented partially summarized or time-averaged data, the data set included short-term flux measurements (e.g., 10−20 min flux values)[54,55] as well as high frequency signals (such as from micrometeorological methods), in part showing unusually large deposition and emission fluxes. For that reason, we removed extreme values based on statistical outlier analysis for each class of measurements (see below), whereby we characterized outliers as fluxes that were more than 1.5 times the interquartile range (IQR) above the third quartile

DOI: 10.1021/acs.est.5b04013
Environ. Sci. Technol. 2016, 50, 507−524

Table 1. Substrate and Air Hg Concentration Definitions, Statistical Values, And Percentile Interval (PI, α = 0.05) for Each Level of Contamination

level	definition		flux (ng m^{-2} h^{-1})								
	substrate Hg (μg g^{-1})	air Hg^0 (ng m^{-3})	mean	standard deviation	median	min	max	PI	n	outliers (%)	ref.
background	≤ 0.3	≤ 3	1.22	2.23	0.70	−4.80	8.10	[−2.90; 6.60]	402	14	14, 17, 21, 24−27, 29, 30, 34, 41, 44−46, 48, 69, 70, 78, 79, 89, 93, 94, 96−98, 105, 107, 126−128, 130, 143, 162−185, 188−190, 193−195
atmospherically influenced		> 3	7.85	12.6	6.60	−18.7	41.7	[−14.9; 32.9]	53	13	18, 25, 36, 45, 53, 82, 183, 195, 196
contaminated	> 0.3		8.54	21.6	1.20	−48.5	102	[−22.9; 75.6]	243	21	18−20, 23, 27, 33, 35, 36, 43, 46, 53, 55, 71, 75, 80, 83, 87, 110, 111, 150, 153, 155, 171, 183, 184, 186, 190, 191, 197−210
naturally enriched			104	141	40.0	−1.90	516	[−0.40; 490]	108	8	25, 40, 50, 51, 60, 70, 73, 211, 212
mining			686	1140	140	−1650	4845	[−17.1; 4150]	289	14	22−24, 26, 48, 50, 54, 55, 70, 72, 73, 203, 210−215

or below the first quartile.[56] This procedure removed 15% of all data from the database, so that our remaining database contained 1094 Hg^0 flux measurements.

We manually entered individual Hg^0 flux measurements, as well as available related auxiliary data, in Access 2013 (Microsoft Corp., Redmond, Washington). We used summary (means, standard deviations, medians, minima, and maxima) and descriptive statistics to synthesize and constrain Hg^0 fluxes from various terrestrial surfaces across a large and diverse global study domain. Because of distribution skewness, we used median values for comparison and a percentile method (α = 0.05) for calculation of confidence intervals. The difference of Hg^0 fluxes between groups of data was determined using Kruskal−Wallis tests (α = 0.05). Linear correlations and Spearman correlation coefficients (ρ) were used to evaluate the influence of controlling factors on Hg^0 flux measurements. We performed all statistical treatments using R 3.2.2 (R Foundation for Statistical Computing, Vienna) and RStudio 0.98 (RStudio Inc., Boston, Massachusetts) and the ggplot2[57] package for density plots (bandwidth = 1); Quantum GIS 2.8 (Quantum GIS Development Team, 2015) was used to map spatial distribution of the study sites using a world map from Natural Earth (naturalearthdata.com).

3. SPATIAL AND TEMPORAL COVERAGE OF HG^0 FLUX MEASUREMENTS

Studies implemented in this database were published between 1977 and 2014 (Figure 1B), including Hg^0 fluxes that ranged from −5493 to 336 000 ng m^{-2} h^{-1} measured across 243 different sites. The sites were unevenly distributed across the world (Figure 1A): most study sites were located in North America (55.6%), Asia (25.1%), and Europe (12.8%); large areas were fully or nearly devoid of Hg^0 flux data, including Africa, Central Asia, Australia, and many polar regions. Sixteen percent of the study sites (and 35% of all flux measurements) were located in naturally enriched zones (i.e., the global mercury mineral belts; Figure 1A),[58,59] in particular along the West Coast of the United States.[42,51,60] Not only were geographical areas differently represented, but measurement types within various geographical regions, also showed large differences in landscapes. For example, North American measurements were dominated by measurements in remote forests and mining sites, in Europe measurements originated mainly from grasslands and contaminated wetlands, and measurements in East Asia were dominated by background grassland as well as contaminated croplands. Given these geographical distribution patterns, it is infeasible to perform an unbiased regional analysis of flux data, thus our spatial analysis focused more on effects of surface cover types than geographic differences. Seventy-five percent of the studies were carried out in the field or under field-like conditions (e.g., mesocosm experiments), and 25% were laboratory studies performed under controlled conditions.

The temporal distribution of measurements also was highly skewed: measurements from spring and summer accounted for half of the total Hg^0 flux measurements, whereas fall and winter together only accounted for 17% of the measurements (Figure 1C). Twenty-eight percent of data did not include sampling times or dates, and 5% of flux measurements were performed across multiple seasons (i.e., long-term measurements). Flux measurements were more heavily focused on daytime (47% of data compared to 13% performed during nighttime; Figure 1D). Thirty-one percent of the data were measurements that lasted for 24-h or longer (i.e., including day- and nighttime), and 9% of the data set was without information about the time of the measurements. Therefore, the assembled data showed that Hg^0 flux measurements were biased both spatially and temporally.

4. MAGNITUDE OF HG^0 FLUXES OVER VARIOUS ENVIRONMENTAL SURFACES

4.1. Hg^0 Flux Magnitudes As a Function of Substrate and Atmospheric Hg Levels. We statistically summarized the magnitude of Hg^0 fluxes measured over terrestrial surfaces with different levels of substrate Hg concentrations. For our examination, we separated measurements into two main classes: background sites and Hg-enriched sites. Background or uncontaminated sites in terrestrial environments previously have been characterized as having substrate Hg concentrations below a range of 0.1−0.5 μg g^{-1},[40,61−65] and some studies have used lower levels (0.01−0.05 μg g^{-1}).[66] We noticed, however, that many studies characterized sites as background based on

DOI: 10.1021/acs.est.5b04013
Environ. Sci. Technol. 2016, 50, 507−524

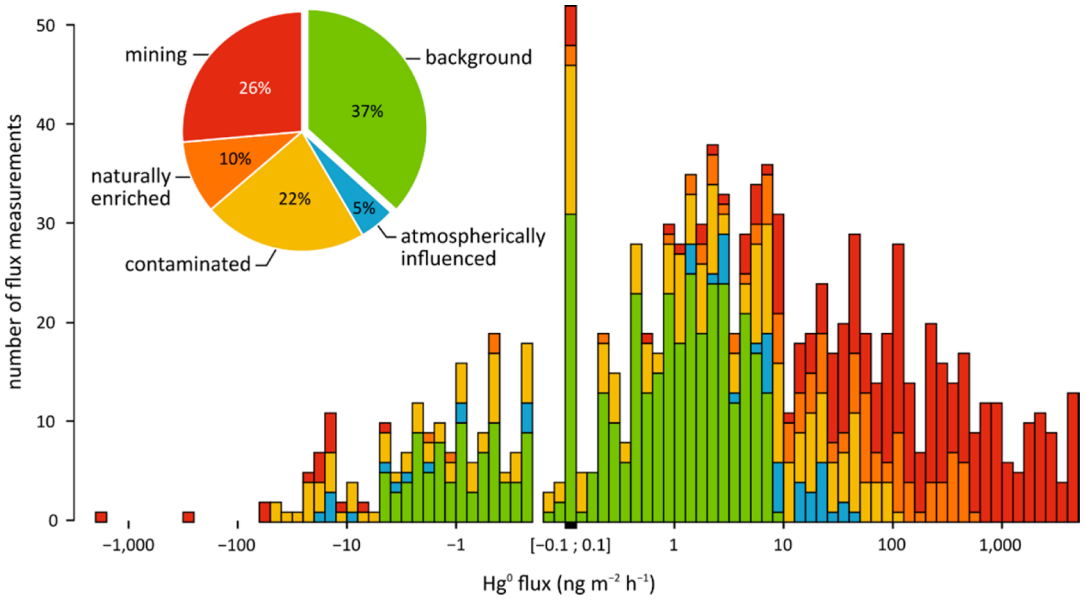

Figure 2. Distribution of Hg^0 fluxes by contamination class (logarithm scale for *x*-axis shows both positive (emission) and negative (deposition) fluxes).

soil Hg concentrations alone, despite some sites having unusually high air Hg^0 concentrations (i.e., well above hemispheric background levels). In addition to substrate Hg concentrations, atmospheric Hg^0 concentrations also have been shown to influence surface−atmosphere Hg^0 exchange (cf. section 5), and therefore such sites would be expected to behave differently compared to true background sites (with low substrate and atmospheric exposure levels).[67] Therefore, we used thresholds both for substrate Hg and atmospheric Hg^0 concentrations to differentiate between background sites and Hg-enriched sites. Based on the range of background concentrations from the literature, background sites in our study were characterized with substrate Hg concentrations ≤0.3 $\mu g\ g^{-1}$. Atmospheric Hg^0 concentrations to delineate sites as background was ≤3 ng m^{-3}, which is about twice the average Hg^0 concentrations commonly observed at background sites. We classified sites as Hg-enriched when either substrate Hg concentrations were >0.3 $\mu g\ g^{-1}$ and/or atmospheric Hg^0 concentrations were >3 ng m^{-3}. Based on this information, we subdivided Hg-enriched sites into four categories: atmospherically influenced (substrate Hg concentration ≤0.3 $\mu g\ g^{-1}$, but atmospheric Hg^0 concentration >3 ng m^{-3}), contaminated (i.e., when anthropogenic pollution was indicated), naturally enriched (such as from the geologic Hg mineral belt and geothermal areas), and mining sites (mainly precious-metal mining such as gold, silver, copper).

Separation of data into these classes revealed a large bias toward Hg^0 flux measurements over Hg-enriched sites (Table 1 and Figure 2), accounting for 63% of all flux measurements; only 37% of all flux measurements were carried out at background sites. Considering that <0.5% of soils across the United States have Hg concentrations >0.3 $\mu g\ g^{-1}$ (based on 4857 soil measurement points in a USGS data set[68]) and assuming similar distributions elsewhere, this suggests that Hg^0 flux measurements over background sites are underrepresented by a factor of about 145 compared to Hg-enriched areas. The relative shortage of Hg^0 flux data from remote background areas that was reported in 1994 by Rasmussen[69] therefore still exists today. The high number of Hg^0 flux measurements in Hg-enriched areas understandably is driven by a particular interest in the contribution of Hg "hot spots" to global atmospheric Hg^0 emissions. At the same time, constraining Hg^0 fluxes over the large majority of global background areas is still challenged by a relative data shortage adding a high level of uncertainty to atmospheric Hg^0 impacts compared to Hg-enriched areas.

Median Hg^0 flux magnitudes from various categories varied significantly in the following order (Table 1 and Figure 2): background < contaminated < atmospherically influenced < naturally enriched < mining areas. The findings of lowest Hg^0 fluxes at background sites and highest Hg^0 fluxes in mining areas were not surprising and are attributed to the well-known influence of substrate concentrations on Hg^0 exchange, with high substrate levels leading to strong stimulation of surface emissions.[26,33,50,51,63,70−74] In fact, mining areas showed by far the highest substrate Hg concentrations in our database, with a median substrate Hg concentration of 30.4 $\mu g\ g^{-1}$, compared to 0.9 $\mu g\ g^{-1}$ in contaminated areas or 0.06 $\mu g\ g^{-1}$ across background sites. Moreover, Hg^0 fluxes measured over mining sites were exclusively performed over bare soils, which typically exhibit higher fluxes than over any other surface (see below).

The magnitude of Hg^0 fluxes also justified defining atmospherically influenced sites, which had median Hg^0 fluxes almost 10 times higher than background sites (Table 1 and Figure 2). We attribute enhanced Hg^0 emissions at these sites to possible surface contamination from high atmospheric Hg^0 exposure. This contamination likely stimulates emission (or re-emission), although the level of contamination may be poorly represented by soil measurements which generally were not enhanced over a threshold value of 0.3 $\mu g\ g^{-1}$. Locations of atmospherically influenced sites were predominantly in East Asia (57%) with 50% of all flux measurements from China showing atmospheric Hg^0 concentrations in the range of 4.0−29 ng m^{-3} (median of 7.6 ng m^{-3} vs 2.3 ng m^{-3} for all other areas).[36,53,75] This observation highlights the severe atmospheric pollution impact in East Asia and its implications for atmospheric Hg^0 emission and re-emissions from these sites.

4.2. Effect of Land Cover and Soil Cover on Hg^0 Exchange. *4.2.1. Land Cover and Soil Cover.* In this section,

DOI: 10.1021/acs.est.5b04013
Environ. Sci. Technol. 2016, 50, 507−524

Table 2. Summary of Hg^0 Fluxes (ng m^{-2} h^{-1}) by Land Cover and Surface: Background (A) and Hg-Enriched (B) Sites

A. background							
land cover	surface type	mean	standard deviation	median	min	max	*n*
forest	bare soil	1.26	1.89	1.00	−2.00	7.58	57
	soil with litter	1.17	1.64	0.70	−1.54	6.98	49
	soil and plant	0.73	2.79	0.70	−4.00	6.00	11
	leaf	−0.06	2.17	0.05	−3.40	2.70	10
	plant	2.96	2.49	2.70	−0.39	5.50	5
	all	1.15	1.97	0.87	−4.00	7.58	132
grassland/shrubland	bare soil	1.40	1.51	1.15	−0.94	4.81	65
	soil with litter	0.18		0.18			1
	soil and plant	0.28	2.82	0.00	−4.30	7.70	31
	leaf	−0.27	0.34	−0.27	−0.51	−0.03	2
	moss	0.08		0.08			1
	all	0.99	2.05	0.60	−4.30	7.70	100
unvegetated land	bare soil	1.63	2.40	0.80	−3.70	8.10	134
cropland	bare soil	0.60	0.85	0.60	0.00	1.20	2
	soil and plant	2.00	1.27	2.00	1.10	2.90	2
	all	1.30	1.20	1.15	0.00	2.90	4
wetland	bare soil	−0.30	0.05	−0.30	−0.33	−0.26	2
	soil and plant	0.32	3.33	0.20	−4.80	6.60	19
	plant	0.90		0.90			1
	water and plant	0.20		0.20			1
	all	0.28	3.02	0.20	−4.80	6.60	23
snow/ice	snow over soil	0.87	2.61	0.40	−2.08	7.40	9
B. Hg-enriched							
land cover	surface type	mean	standard deviation	median	min	max	*n*
forest	bare soil	8.38	7.61	7.15	1.28	22.9	6
	soil with litter	3.35	4.99	0.55	−0.50	16.0	14
	soil and plant	24.8	39.9	13.5	−25.0	93.0	20
	leaf	0.37	18.1	−0.07	−48.5	92.7	78
	plant	−9.00		−9.00			1
	all	5.15	23.6	0.01	−48.5	93.0	119
grassland/shrubland	bare soil	67.5	48.5	67.5	33.2	101.8	2
	soil and plant	4.04	10.2	2.20	−18.7	30.0	16
	moss	1.50		1.50			1
	all	10.6	24.9	2.50	−18.7	101.8	19
unvegetated land	contaminated bare soil	55.7	243	7.78	−61.9	2330	176
	geothermal area	210	167	142	12.0	677	50
	rock	42.9	52.5	42.9	5.70	80.0	2
	all	89.5	236	14.1	−61.9	2330	228
man-made surfaces	mining area	824	1220	245	−1650	4845	230
	urban area	1.33	1.93	0.70	0.02	6.50	13
	waste	8.35	14.1	7.12	−18.78	41.0	28
	all	700	1160	140	−1650	4845	271
cropland	bare soil	20.1	18.3	18.2	−4.10	75.6	35
	soil and plant	25.7	26.4	17.3	−3.10	77.1	9
	all	21.2	20.0	17.8	−4.10	77.1	44
wetland	bare soil	42.7		42.7			1
	plant	10.5	9.90	10.5	3.50	17.5	2
	water and plant	3.56	6.47	1.80	−3.30	13.5	5
	all	10.2	14.8	5.00	−3.30	42.7	8
snow/ice	snow over soil	6.74	3.98	8.01	0.95	10.0	4

we further categorized background and Hg-enriched sites by their dominant land cover types (Table 2). We identified six land cover types for background sites and seven for Hg-enriched sites (specified in Table 2A and B, respectively). Within each land cover classification, we further identified the specific surfaces of flux measurements as follows: if data included measurements made over bare soils (vegetation-free sites plus soil surfaces not covered by litter or snow), soils covered by litter, and measurements made over plant surfaces (i.e., individual leaves or leaves plus branches).

In the next section, we first focused on discussing Hg^0 fluxes for bare soil surfaces and compared these across different sites and across different land cover types, and later included other surfaces. Bare soil measurements accounted for the majority of all Hg^0 flux measurements both in Hg-enriched (80%) and background (65%) categories, whereas measurements over

DOI: 10.1021/acs.est.5b04013
Environ. Sci. Technol. 2016, 50, 507−524

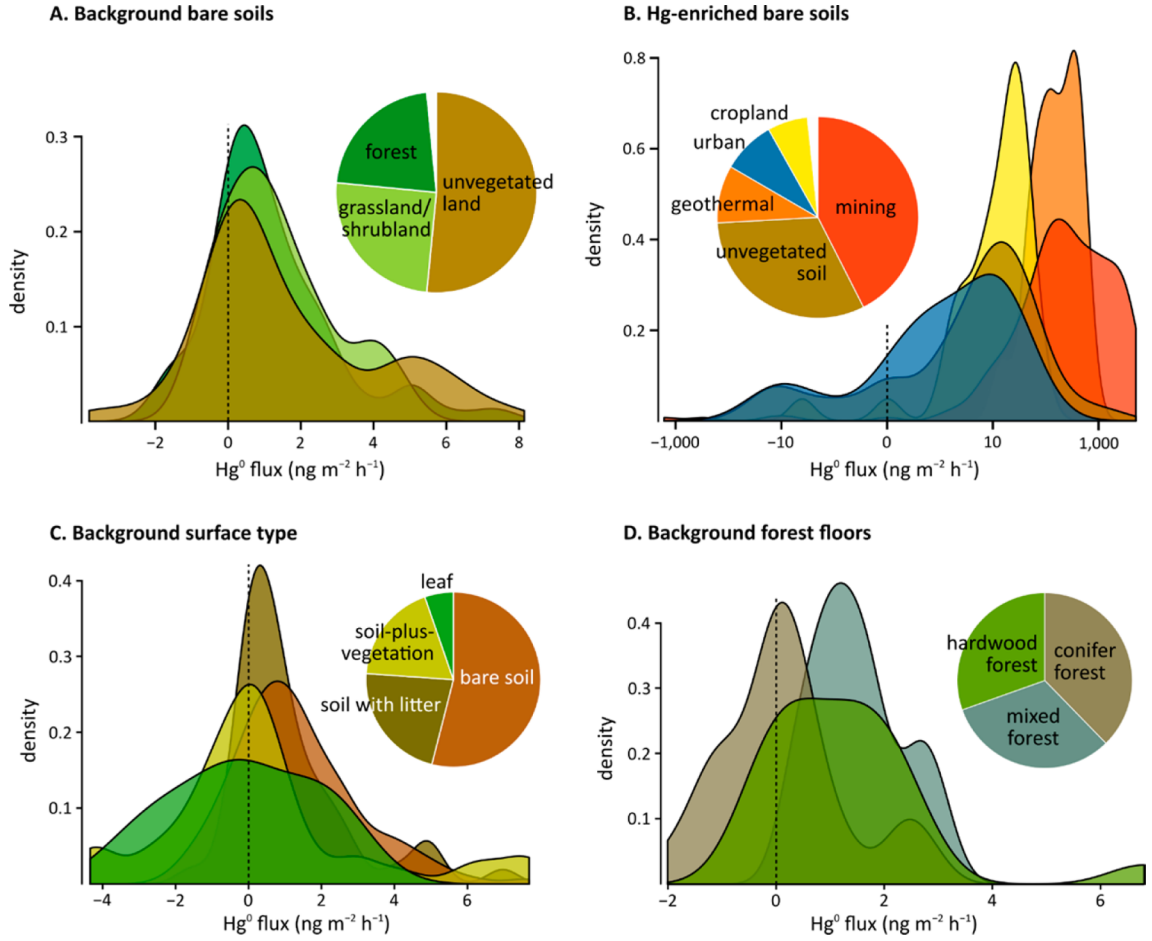

Figure 3. Distribution density of Hg^0 fluxes from background (**A**) and Hg-enriched (**B**) bare soils by land cover ($n > 10$), background surfaces by vegetation cover type (**C**), and background forest floors by forest type (**D**). Only classes with $n > 10$ are presented.

other surfaces (in particular vegetated surfaces) were underrepresented.

4.2.2. Bare Soil Hg^0 Fluxes Across Different Landscapes. We ranked Hg^0 fluxes reported from bare soils in background areas (Table 2A and Figure 3A) in the following order: wetland soils < cropland soils < soils in unvegetated areas < forest soils < grassland/shrubland soils (note that bare soil measurements existed in all land cover types, including on bare soil "patches" in grasslands or forest floors). Wetland fluxes are not discussed further here since we aimed to focus on terrestrial surfaces and processes. Land use categories for bare soils showed dominant emission of Hg^0 to the atmosphere, but to our surprise, fluxes over soils at unvegetated sites (i.e., open areas) were on average 25% lower than soils located under canopies (i.e., forests and grasslands/shrublands). Bare soil fluxes measured over grasslands/shrublands exceeded fluxes in forests, although none of these differences were statistically significant ($p = 0.464$). Previous comparisons of fluxes measured over forested and nonforested soils showed higher Hg^0 emissions over grassland soils compared to forest and unvegetated soils (by a factor of 2−3.5).[31,53] Vegetation and plant canopies shade underlying soils, with forest canopies absorbing up to 99% of the solar radiation load.[76−78] Canopy covers in forests and grasslands/shrublands, therefore, are expected to reduce Hg^0 emissions by limiting soil warming and solar loads. The lack of significant flux differences and even a slight trend toward higher Hg^0 emission fluxes over bare soils in forests and grasslands as opposed to open areas may be due to high between-site variability, so that differences and effects attributable to individual factors (such as shading) were smaller than the variability found across sites in the large global data set. Other reasons for observed patterns, however, may well include the fact that soils under vegetation show up to 2.5 times higher substrate Hg concentrations compared to unvegetated bare soils (attributable to plant-derived Hg deposition),[79] which may promote soil Hg^0 emission fluxes and compensate for a potential reduction in fluxes due to shading.

We ranked median Hg^0 fluxes from Hg-enriched bare soils and surfaces (Table 2B and Figure 3B) in the following order: forest soils < cropland soils < wetland soils < grassland/shrubland soils < urban surfaces < soils in geothermal areas < mining soils. Mining and geothermal areas showed significantly higher fluxes compared to all other soils ($p < 0.001$; e.g., exceeding other fluxes by a factor of 2−350). As mentioned above, the large difference for mining sites is related to their very high substrate Hg concentrations (mean of 226 $\mu g\ g^{-1}$) compared to all other Hg-enriched sites (mean of 17.8 $\mu g\ g^{-1}$), and at times exceptionally high Hg^0 emissions from mining areas reflect the importance of such point-source contributions for atmospheric Hg^0 loads as has been reported and discussed in many publications.[22,26,55,80] For Hg-enriched sites, we observed the expected patterns that soils under forest canopies have the lowest Hg^0 fluxes compared to all other categories. We found in the Hg-enriched category, forested sites did not show

DOI: 10.1021/acs.est.5b04013
Environ. Sci. Technol. 2016, 50, 507−524

higher soil Hg concentrations compared to open bare soil locations, so that the observed patterns may in fact reflect the role of solar radiation in promoting Hg^0 emissions across Hg-enriched sites in unvegetated and sun-exposed sites.

4.2.3. Effect of Soil Cover and Ecosystem Structure. We further evaluated the influence of soil cover (e.g., litter, snow, and plant) on Hg^0 fluxes by comparing measurements from bare soil with those from soil covered by litter, soil covered by snow, over plant or leaf surfaces only, and sites including soils-plus-vegetation (i.e., whole ecosystem level fluxes). We focused this analysis on background forested and grassland/shrubland sites, as well as snow surfaces, where most of such measurements were available (Figure 3C). Based on median values, measured Hg^0 fluxes increased in the following order: plant/leave surfaces (−0.12 ng m^{-2} h^{-1}, n = 12) < soil-plus-vegetation (0.00 ng m^{-2} h^{-1}, n = 42) < soil covered by snow (0.40 ng m^{-2} h^{-1}, n = 9) < soil covered by litter (0.70 ng m^{-2} h^{-1}, n = 50) < bare soil (1.07 ng m^{-2} h^{-1}, n = 122). Fluxes from bare soils were significantly higher than soil-plus-vegetation (p < 0.05), as well as from soils covered by plants and litter (p < 0.01). We interpret these patterns as indicating that the presence of any soil cover decreases atmospheric Hg^0 fluxes compared to bare soils only, and even leads to a shift from a net atmospheric emission to a net deposition from the atmosphere, although absolute flux differences were relatively small (<1 ng m^{-2} h^{-1}).[81,82]

Vegetation is known to contribute to Hg^0 flux exchange, most importantly constituting a sink for atmospheric Hg^0,[83,84] including through stomatal uptake[33] and other dry deposition processes.[85] The important role of leaves as a sink is supported by exposure studies that showed increasing leaf Hg concentrations under higher atmospheric Hg^0 exposures.[18,45,86,87] The resulting effects are that vegetated ecosystems increase atmospheric deposition compared to open areas through additional litterfall and throughfall deposition,[67,88−92] and such plant depositions are now recognized to contribute the majority of Hg accumulating in soils at many sites.[79,93,94] Analyzing Hg^0 exchange from foliar surfaces in our database, however, showed foliar fluxes spanning a much larger range compared to any other surface (Figure 3C) − from deposition (−3.40 ng m^{-2} h^{-1}) to emission (2.70 ng m^{-2} h^{-1}) with an IQR of 3.13 ng m^{-2} h^{-1} (compared to IQRs of 2.12 and 1.37 ng m^{-2} h^{-1} for bare soil and litter-covered soils, respectively).[18,33,83,95] We attribute this large flux range to (1) a low number of foliar flux measurements conducted under background conditions, with only 12 flux measurements from four studies;[18,33,83,95] and (2) difficulties and possibly serious methodological problems in measuring leaf-atmosphere Hg^0 exchange, with studies employing different chamber methods with different designs and turnover rates. Our analysis suggests that foliar−atmosphere exchange of Hg^0 has the highest uncertainty of all terrestrial fluxes. The shortage of reliable foliar flux data is particularly concerning given that leaf areas are several times higher than soil surface areas, with leaf area indices ranging from 3.1 to 6.9 in forests and from 1.7 to 2.5 in grasslands/shrublands,[96] and the uncertainty in understanding foliar-atmosphere exchange fluxes leads to large uncertainties in estimating worldwide terrestrial−atmosphere exchange (cf. section 7).

Although absolute flux differences between bare soils and soil-plus-vegetation systems were small, it is noteworthy that the presence of vegetation led to a substantial shift in the percentage of fluxes experiencing net Hg^0 emission vs net Hg^0 deposition. For example, only 20% of bare soil measurements conducted in forests and grasslands/shrublands showed net deposition, while this percentage increased to 48% when vegetation was included in measurements. This finding was consistent with a flux partitioning study over grasslands in a greenhouse facility showing that soil emissions were partially intercepted and offset by overlying vegetation, resulting in lower whole-ecosystem fluxes compared to bare soils only.[95] A key issue with available fluxes is that whole-ecosystem flux data (i.e., combined soil-vegetation measurements that integrate all fluxes over a representative vegetated surface) represented only 18% of all available fluxes, and that these studies were generally limited to grasslands/shrublands. This is due to limitations in available measurement methodology that is difficult to apply over forests (cf. section 6). We propose an urgent need for better characterization of whole-ecosystem fluxes, including different ecosystem types and, in particular, forests. In addition, better characterization of the role of leaves and plants in net Hg^0 exchange is needed under undisturbed natural conditions to reduce current uncertainties in Hg^0 exchange from vegetated terrestrial ecosystems.

Our database further indicates lower Hg^0 emissions from evergreen coniferous forest floors including bare soils and litter-covered soils (median of 0.07 ng m^{-2} h^{-1}, n = 26) compared to deciduous broadleaved forests (1.40 ng m^{-2} h^{-1}, n = 21, p < 0.05) and mixed deciduous-conifer forests (1.50 ng m^{-2} h^{-1}, n = 22, p < 0.001), as reported elsewhere (Figure 3D).[97,98] Generally higher total Hg deposition is observed in evergreen forests due to increased canopy scavenging[99−103] and differences in ecophysiological features between deciduous and conifer trees (e.g., stomata density, stomatal conductance, carbon fixation[98,104,105]); but this higher deposition apparently does not result in increased forest floor re-emission of Hg^0.

Several field studies[49,50] show that Hg^0 fluxes over litter-covered forest floors are lower compared to bare soils−as seen in our database as well−and this has been attributed to shading of soil surfaces.[34,50] Alternatively, forest litter studies[106−109] also show that gaseous Hg^0 emission occurs from litter, in the range of 10−20% of the amount contained in litter is possibly re-emitted in the first year, a finding which seemingly contradicts the above patterns. We suggest that under undisturbed field conditions, the potential Hg^0 source from litter is smaller than the impact of shielding soils from direct atmospheric contact (e.g., solar radiation and temperatures), thereby reducing soil Hg^0 emissions.[29,34,110,111] A recent publication focusing on soil pore Hg^0 measurements further suggests that soil Hg^0 emissions originate from the very top of the soil profile, while the rest of the profile constitutes an Hg^0 sink.[112] Therefore, it is possible that shading and coverage of soils affect emissions directly at the surface, but with little or no effects deeper in the soil matrix.

As observed for vegetation, snow-cover negatively influenced soil Hg^0 emissions compared to bare soils (Table 2A). This supports that the presence of a snowpack decreases net Hg^0 emissions compared to bare soils, despite an important role in photoreduction of Hg^{II} and losses of Hg^0 from snowpack driven by solar radiation.[113,114]

5. FACTORS CONTROLLING HG^0 EXCHANGE

Many studies have identified factors that correlate with the magnitude and direction of surface−atmosphere Hg^0 exchange−including atmospheric, chemical, and physical parameters (Table S1, Supporting Information). The most common

DOI: 10.1021/acs.est.5b04013
Environ. Sci. Technol. 2016, 50, 507−524

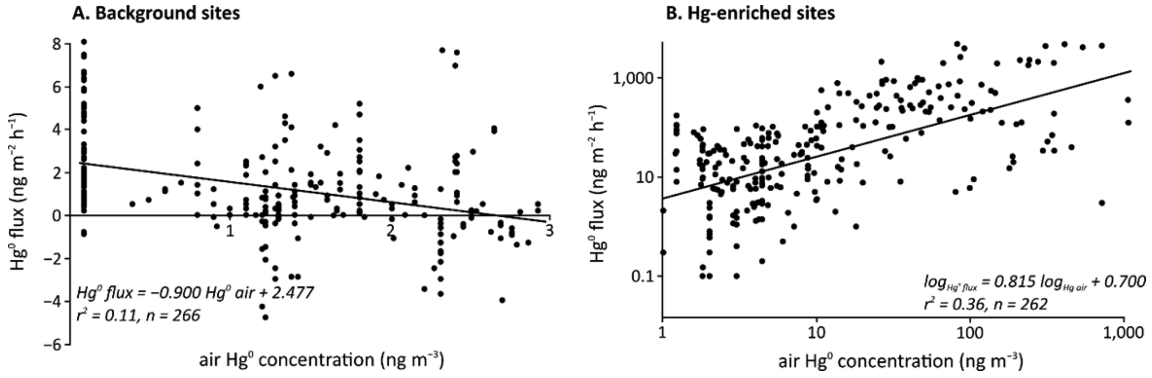

Figure 4. Hg^0 flux vs air Hg^0 concentration relationship: background (**A**) and Hg-enriched (**B**) sites.

and pronounced Hg^0 relationship was with solar radiation that was reported in the literature in a total of 65 cases with positive correlations. This relationship often is attributed to photochemically mediated reduction that converts soil Hg^{II} to volatile Hg^0,[37,47,110,115−119] although other biotic and abiotic processes also contribute to Hg^{II} reduction—including reduction by humic acids[120,121] and iron oxides under anoxic conditions[122] as well as reduction by microorganisms[123−127] and/or microbial exudates.[102,128,129] Other important correlations were identified with soil and air temperatures (47 and 45 cases with positive correlations, respectively), which often is collinear to radiation, but also may be linked directly to activation energy of Hg^0,[32,43,48,55] or stimulation by soil microbial activity.[55,130] Another relationship frequently found in the literature (29 cases of correlations) was with substrate Hg concentrations, which consistently and positively correlated to Hg^0 fluxes over terrestrial surfaces.

When calculating Spearman coefficient correlations between these variables and Hg^0 fluxes across the entire database (as opposed to the study observations; Table S1, Supporting Information), most of the correlations disappeared, with the exception of a significant correlation remaining for substrate Hg concentration ($\rho = 0.633$, $p < 0.001$, $n = 945$). Reasons for this likely include strong differences in flux magnitudes and strong intersite variability (such as differences in environmental conditions and vegetation),[60] as well as potentially different measurement methodologies. While use of stepwise or hierarchical regression models would allow us to partially attribute a large component of the overall variability to individual factors, the lack of a comprehensive set of variables measured across all studies renders this technique infeasible with the data from our database. This translates into similar challenges in developing process-based or hierarchical models to calculate surface−atmosphere fluxes across multiple sites since it remains unclear to what degree controls observed at individual sites are applicable across large areas.

In the following two sections, we further characterize controlling factors separately for background and Hg-enriched sites to evaluate their importance in subsets of data under high (Hg-enriched) and low (background) Hg^0 flux conditions. An apparent and surprising finding using all data from the database as well as separated data (Hg-enriched and background data sets) was an absence of seasonality in Hg^0 fluxes (i.e., spring/summer/fall/winter), as well as a lack of daytime and nighttime Hg^0 flux differences (Figure S2, Supporting Information). This is in contrast to studies that have reported strong seasonality in Hg^0 flux measurements at individual sites,[30,52,53,131] as well as strong diurnal patterns of fluxes such as near-Gaussian increase in fluxes along with daytime solar radiation.[22,41,132,133] Others, however, also reported an absence of diurnal patterns over vegetated sites (mainly at the whole-ecosystem level over grasslands), as well as an increase of deposition fluxes in summer opposing often reported stimulatory effects of solar radiation and temperature on Hg emissions.[82,134] These results suggest that high variability of Hg^0 fluxes across sites, as well as potentially different impacts of environmental parameters in different ecosystems (e.g., vegetated vs bare soils) are greatly complicating the analysis of controlling variables that are evident during measurements at individual, well-constrained sites.

5.1. Factors Controlling Hg^0 Fluxes in Background Sites. Across all background soils (bare, litter-covered, and plant-covered), a key finding was an apparent lack of correlation between substrate Hg concentrations and Hg^0 fluxes ($\rho = -0.085$, $p > 0.05$, $n = 307$), indicating either little control of substrate concentration on Hg^0 fluxes across background sites, or that other variables prevailed over the effects of substrate Hg concentration. This finding possibly was related to the fact that background sites showed a much narrower range of soil Hg concentrations compared to Hg-enriched substrates where such effects were clearly present (cf. section 5.2), although other studies have observed positive correlations between substrate Hg concentrations and fluxes across individual sites.[25,74] Similarly, others have observed predictable influences of environmental variables on Hg^0 exchange across multiple sites when using consistent measurement methodology, such as correlations with solar radiation, air temperature, or relative humidity.[38,82,111,135] For example, Kuiken et al.[82] reported that solar radiation and air Hg^0 concentrations were the main variables controlling Hg^0 fluxes for six sampling sites in the eastern United States, while Ericksen et al.[31] found across 46 background sites with different land covers that soil moisture was an important environmental parameter. We propose that reasons for this lack of correlation may include high between-site heterogeneity due to different landscapes and surface properties (e.g., open areas, vegetated areas, shading by plants) as well as different measurement methodologies. Ericksen et al.,[31] however, also showed that correlations to environmental variables change significantly across different sites, suggesting that environmental controls on Hg^0 fluxes in fact vary between sites.

Nevertheless, atmospheric Hg^0 concentration was significantly correlated with Hg^0 exchange in background sites across all soil data ($\rho = -0.312$, $p < 0.001$, $n = 263$). Hanson et al.[45] first described the presence of an atmospheric compensation point for Hg^0 fluxes, that was characterized as a threshold air

DOI: 10.1021/acs.est.5b04013
Environ. Sci. Technol. 2016, 50, 507−524

concentration where Hg^0 fluxes switch from net deposition (at high Hg^0 exposures) to net emission (at low Hg^0 exposure). Over soils, laboratory studies have shown compensation points in the range of 0.1−25 ng m^{-3},[18,45,136] and compensation points also have been reported over foliage in the range of 0.6−3 ng m^{-3},[48,131,137,138] implying that both soils and vegetation can serve either as net emission sources or net deposition surfaces depending on atmospheric conditions. The linear regression between Hg^0 fluxes and air Hg^0 concentrations (Figure 4A) was

$$Hg^0_{flux} = -0.900 Hg^0_{air} + 2.477 (r^2 = 0.11, n = 266) \quad (1)$$

The calculated compensation point across background sites in our database combining both soil (barren and litter-covered soils) and soil-plus-vegetation measurements was 2.75 ng m^{-3}, which was high compared to 1.0−1.7 ng m^{-3} for the background atmospheric level.[3−5] The compensation points observed and derived mainly from laboratory studies were in a similar range with data from this database, consisting mainly of field measurements.

Finally, a variable that surprisingly was correlated with Hg^0 fluxes across background sites was soil pH (ρ = 0.335, p < 0.001, n = 113). This also was evident by the fact that only 29% of soils with pH < 5 showed net Hg^0 emission, whereas 87% of measurements with a soil pH > 5 showed net Hg^0 emissions. Soil pH is an important factor for the chemistry of metals, including Hg, influencing their adsorption, complexation, dissolution, speciation, and retention on mineral and organic particles,[139−142] as well as affecting microbial processes that also can control Hg^0 fluxes.[43,129,143−148] Furthermore, soil pH can differ among different ecosystem types, (e.g., generally lower soil pH in coniferous ecosystems), which may contribute to such relationships, although no inherent flux differences were observed between coniferous and deciduous forest floors as discussed above. We therefore recommend further study of the pH-dependence of Hg^0 fluxes in the field to understand the controls of soil chemical factors, such as pH, on volatility and emission behavior of Hg^0.

5.2. Factors Controlling Hg^0 Fluxes in Hg-Enriched Sites. Substrate Hg concentrations exerted a dominant control on Hg^0 emission across data from Hg-enriched sites (ρ = 0.608, p < 0.001, n = 538). High substrate Hg concentrations, as found in these Hg-enriched sites, clearly lead to a well-known strong enhancement of surface Hg^0 emissions.[26,33,50,51,63,70−74] A linear regression between Hg^0 fluxes and substrate Hg concentrations (Figure 5) showed the following relationship:

$$\log_{Hgflux} = 0.427 \log_{Hgsoil} + 1.432 (r^2 = 0.26, n = 381) \quad (2)$$

The slope is in the same order of magnitude as slopes reported in the literature for specific Hg-enriched regions, in the range of 0.51−0.68.[50,63,65] Therefore, across a diverse group of Hg-enriched sites, substrate Hg concentrations were found to be an important and consistent factor that explained a substantial amount of the variability in observed Hg^0 emission fluxes.

At Hg-enriched sites, atmospheric Hg^0 concentrations also were significantly and—in contrast to background sites—positively correlated to Hg^0 fluxes (ρ = 0.409, p < 0.001, n = 321), showing the following relationship (Figure 4B):

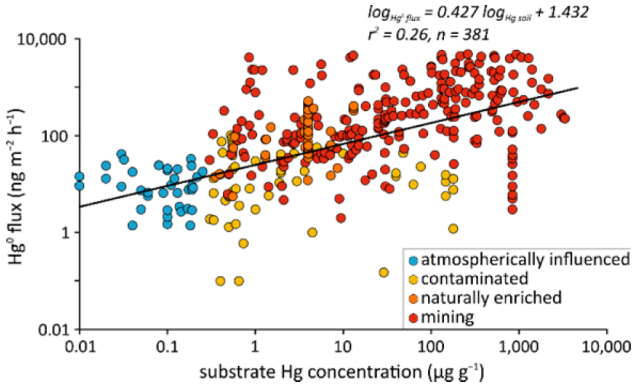

Figure 5. Hg^0 flux vs substrate Hg concentration relationship for Hg-enriched sites.

$$\log_{Hg^0flux} = 0.815 \log_{Hg\,air} + 0.700 (r^2 = 0.36, n = 262) \quad (3)$$

The positive correlation also was in contrast to the concept of a compensation point. We attribute the correlation to particularly high Hg^0 emission at some Hg-enriched sites which leads to a buildup of Hg^0 near the surface in the boundary layer. Therefore, the relationships were likely caused by high surface emissions leading to high atmospheric Hg^0 concentrations, and not vice versa via a control of air Hg^0 concentration on Hg^0 exchange fluxes. This observation also could be the reason that across individual studies, both negative and positive correlations between atmospheric Hg^0 concentrations and fluxes were reported (Table S1, Supporting Information).

Finally, across all Hg-enriched soil and soil-plus-vegetation data, soil moisture showed a small negative influence on Hg^0 emissions across Hg-enriched sites (ρ = −0.267, p < 0.01, n = 60). This pattern is in contrast to the majority of studies that reported positive correlations between soil moisture and emission of Hg^0,[29,43,47,81,149] although a few studies also showed negative correlations.[95,150] It has been proposed that soil water promotes Hg^0 desorption from soil particles into soil pores, and that soil water evaporation facilitates Hg mobilization toward the soil surface and atmospheric release.[44]

6. METHODOLOGICAL BIAS

Measurements of Hg^0 fluxes from terrestrial environments are primarily based on two measurement methodologies (cf. SI 1, Supporting Information). First, dynamic flux chambers (DFC) have been used for the majority of flux measurements (85%) and are based on comparisons between inlet and outlet air Hg^0 concentration measurements in a chamber placed over a specific surface area.[21,151,152] The second type, micrometeorological (MM) approaches, are based on measurements of vertical concentration gradients above the surface coupled with characterizations of atmospheric turbulence.[43,153] Direct comparisons between these two methods at individual sites highlight a potentially large influence of the employed method on Hg^0 flux measurements.[60,154,155] Each method presents its own benefits and drawbacks related to application, and we discuss these issues in detail in the Supporting Information. The DFC method, for example, disturbs the system under measurement (e.g., inside temperature may be quite different from outside chamber temperature) and the limited footprint of measurements make scaling up fluxes to the ecosystem level for comparisons difficult. Alternatively, with current MM

DOI: 10.1021/acs.est.5b04013
Environ. Sci. Technol. 2016, 50, 507−524

technologies, background sites are often at or near detection limits, and measurements need to be time-averaged to detect fluxes.

We assessed if the methodology used to measure Hg^0 fluxes may induce a bias across our large global data set, focusing on background sites to limit flux heterogeneity. Hg^0 fluxes measured by the MM method (median of −0.01 ng m^{-2} h^{-1}, n = 51) were significantly lower (p < 0.001) than DFC measurements (median of 0.90 ng m^{-2} h^{-1}, n = 300) across background data (including bare soils, litter-covered soils, and soil-plus-vegetation), raising concerns in regards to an overestimation of fluxes based on DFC compared to MM measurements. The discrepancy, however, could also result from site footprint heterogeneity (i.e., typically 0.03−0.5 m^2 for DFC vs 10−100 m^2 for MM approaches) or different method sensitivity. Another reason may include different representations of ecosystem types between these methods: for example, 98% of MM measurements included vegetation whereas only 4% of DFC measurements were performed over whole ecosystems. Therefore, to compare DFC with MM requires careful characterization of different footprints, including variability in surface conditions and presence of vegetation.

Many studies reported the influence of DFC design and operation on Hg^0 flux measurements (e.g., chamber shape,[154,157] chamber material,[158] or flushing flow rate[42,159,160]). Comparisons performed using background data showed that rectangular DFCs (median of 1.1 ng m^{-2} h^{-1}, n = 90) recorded significantly higher (p < 0.01) Hg^0 fluxes than semicylindrical designs (median of 0.3 ng m^{-2} h^{-1}, n = 125), probably due to the nonhorizontal flow observed in the semicylindrical DFC reducing the exchange surface area. Another important design parameter is the DFC material: measurements obtained using polycarbonate chambers (n = 154) in background environments were statistically lower (p < 0.001) than those from Pyrex (n = 65) and Teflon (n = 52) chambers (medians of 0.40, 2.00, and 1.80 ng m^{-2} h^{-1}, respectively). These observations were consistent with the literature which related such differences to incident light: polycarbonate chambers block wavelengths <320 nm, which then leads to underestimation of the Hg^0 flux measurements.[158] The low number of quartz DFC (median of 1.40 ng m^{-2} h^{-1}, n = 29) did not allow us to see any statistical difference or to confirm observations by Edwards and Howard[48] reporting best UV transmittance of this material.

Air flow rate inside the chamber also influences exchange of Hg^0, and we observed that DFC measurements using a flushing flow rate ≤2 L min^{-1} (median of 0.5 ng m^{-2} h^{-1}, n = 152) were significantly lower (p < 0.001) than those obtained using a flow rate >2 L min^{-1} (median of 1.75 ng m^{-2} h^{-1}, n = 148; Figure 6, Supporting Information). A similar effect was observed when comparing chamber turnover rate (data not shown, less data available). Some scientists suggest using a high flushing flow rate (>15 L min^{-1}) to limit a possible underestimation of fluxes,[157,160] particularly for Hg^0 exchange over Hg-enriched substrate.[154] Others, however, recommended using low flushing flow rates (<1.5 L min^{-1}) at background sites.[154,161] Indeed, elevated flushing flow rates may create an artificial Hg^0 flux from the soil by generating a partial vacuum inside the chamber.[42,161] Our observations support this assumption: measurements using DFC with high flow rate were farther apart (p < 0.001) from MM measurements (median of −0.01 ng m^{-2} h^{-1}, n = 51) than measurements using DFCs with low flow rates (p < 0.05), assuming that MM measurements best represent natural conditions in the field without effects of chamber designs or operation procedures on fluxes.

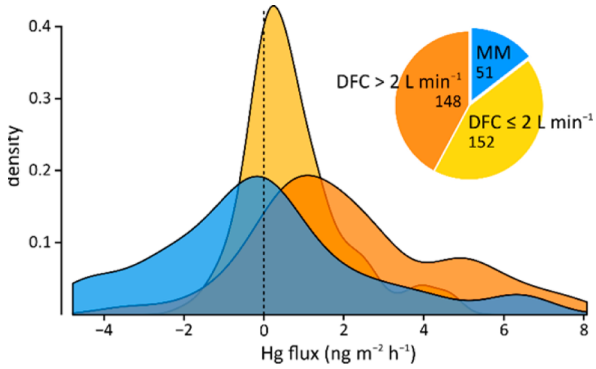

Figure 6. Methodological influence on Hg^0 flux measurements in background sites: distributions obtained by MM, DFC with a flushing flow rate ≤2 L min^{-1}, and DFC with a flushing flow rate >2 L min^{-1}.

The quality control of DFC Hg^0 flux measurement is evaluated by characterization of a chamber blank, generally sealing a clean chamber with a clean sheet in the laboratory and/or under field conditions.[26,60,111] Our database statistics showed that blank measurements were performed for 63% of DFC data, and values for blanks were published in 77% of these cases, so that only 49% of all DFC data reported DFC blanks. Even more concerning is that only 14% of DFC flux measurements were blank corrected (i.e., blank data were subtracted from measurements), which likely constitutes another bias of measurements when comparing different studies as well as different methodologies. We strongly recommend standardization of chamber design and operating procedures that are currently not in place for these methods,[63] as well as careful reporting of operating procedures (blanks, flow, chamber turnover rates, etc.) to facilitate intercomparison of measurements performed using different methodologies.

7. CONSTRAINING HG^0 FLUXES USING STATISTICAL FLUX DISTRIBUTIONS FROM DIFFERENT LANDSCAPES

Models have been used to estimate that emission and reemission from terrestrial surfaces may account for 50% or more of present-day Hg^0 emissions, that are globally in the range of 1000−2200 Mg·a^{-1}.[15−17,162,163] Most studies in our database were campaign studies attempting to elucidate the magnitude as well as controlling influences on the surface−atmosphere Hg^0 exchange to further our understanding of these exchange processes. While quantifying the effects of various controlling factors presents the opportunity to develop process-based or empirical models to scale up fluxes from small footprints and individual sites to regional and global-scales, our database analysis showed that many relationships observed at individual sites were lost when considered across sites. As discussed above, this potentially was due to different environmental controls across sites, large spatial and temporal variability of fluxes, as well as possible issues with comparable measurement methodologies, thereby constituting a major problem in scaling up fluxes based on such determining variables.

Instead, in our study we estimated global surface−atmosphere Hg^0 exchange by extrapolating the best statistical distribution of fluxes from different land covers and surfaces instead (as done, for example, for smaller areas such as the Great Lakes region in the United States[164]). Since no significant

DOI: 10.1021/acs.est.5b04013
Environ. Sci. Technol. 2016, 50, 507−524

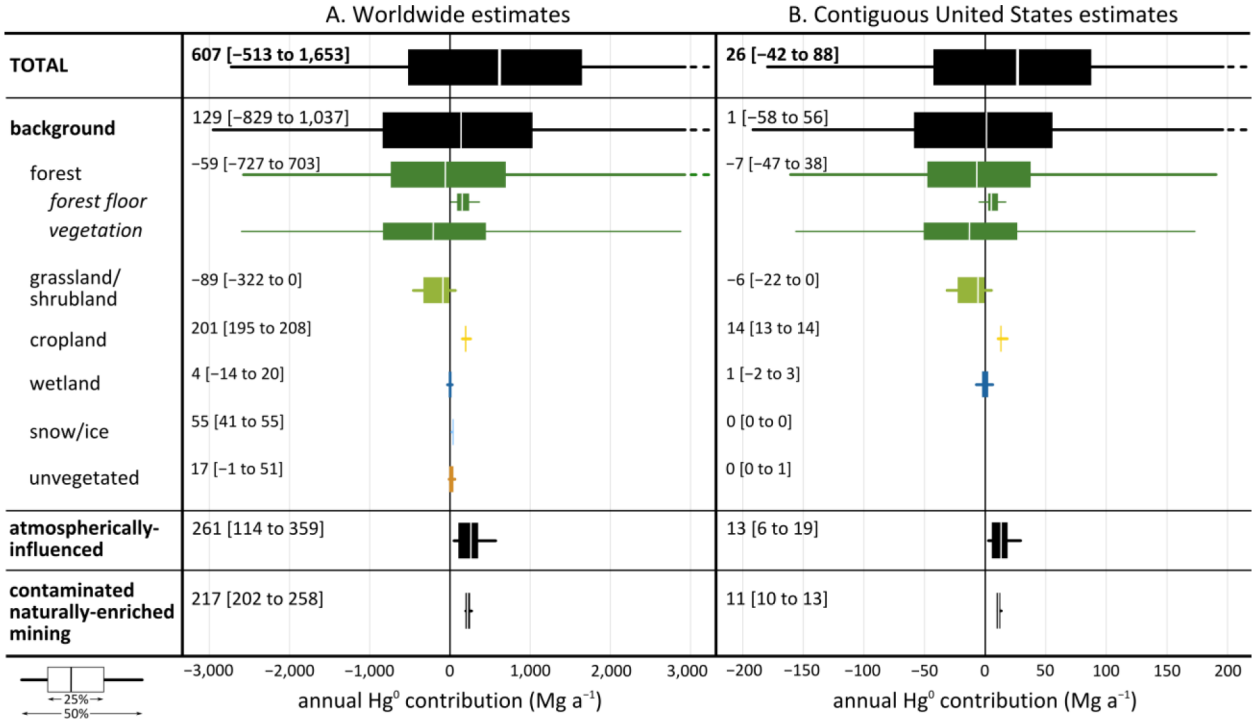

Figure 7. Global annual estimates of Hg^0 exchange ($Mg \cdot a^{-1}$) over terrestrial surfaces across different land covers: worldwide (**A**) and the contiguous United States (**B**). Positive values signify emissions, and negative values signify deposition. Numbers indicate medians and uncertainty ranges between 37.5th and 62.5th percentiles. Background represents the sum of six subcategories (forest, grassland/shrubland, cropland, wetland, snow/ice, and unvegetated (i.e., bare soils). Forest fluxes were calculated based on forest floor Hg^0 flux measurements and leaf fluxes multiplied by leaf area indices since whole-ecosystem forest fluxes are largely missing in the literature.

trends were observed for different seasons or time of day (cf. section 5 and Figure S2, Supporting Information), we refrained from adjusting flux measurements using diel Gaussian flux patterns as frequently performed in the literature.[22,25,50,65,135] We used fluxes based on MM measurements, as well as DFC measurements operated at low flow rates including data collected under many different environmental conditions (e.g., day- and nighttime measurements, different seasons, various temperatures), although the conditions were clearly not evenly distributed nor a quantitatively represention of the conditions across the entire scaling area. For our estimate, median Hg^0 fluxes −37.5th and 62.5th percentiles, as well as the 25th and 75th percentiles are presented to show uncertainty ranges of estimates−were calculated as follows (cf. SI 2, Supporting Information): bare soils fluxes were used for unvegetated areas; soil-plus-vegetation were applied to grasslands/shrublands, croplands, and wetlands; and fluxes from snow-covered soils were used for snow- and ice-covered areas. Due to a dearth of measurements over whole forest ecosystems, we calculated forest fluxes based on forest floor measurements (including bare soils and litter-covered soils) and estimated foliar fluxes by means of forest leaf fluxes multiplied in addition by respective forest leaf area indices[96] for hardwood, conifer, and mixed forests. We used various models of land surface for both worldwide and contiguous United States: GLC 2000, GLC-SHARE 1.0, GLCC 2.0, MODIS, and NLCD 2011.[165−167] We estimated that 0.5% of the global terrestrial land surface is characterized as Hg-enriched (contaminated, naturally enriched, and mining, with Hg concentration >0.3 $\mu g\ g^{-1}$) which is based on a recent geochemical data set for soils in the United States.[68] For Hg-enriched sites, we used the linear equation from the relationship between Hg^0 fluxes and substrate Hg concentrations (eq 2) applied to the frequency distribution of Hg-enriched soil concentrations (>0.3 $\mu g\ g^{-1}$) in the soil data set of the United States and applied this both for worldwide and contiguous United States flux estimates.[68] The area representing "atmospherically-influenced" sites was estimated at 3% based on Hg^0 atmospheric concentrations (>3 ng m^{-3}) from the Community Atmosphere Model with Chemistry (CAM-Chem)/Hg model.[168]

Global (Figure 7A) and contiguous United States (Figure 7B) median estimates for Hg^0 exchange fluxes from different landscapes are shown with uncertainty ranges (between 37.5th and 62.5th percentiles in boxes in the figure, and given in square brackets in the text; between 25th and 75th percentiles lines in the figure). The estimated total worldwide annual Hg^0 contribution from terrestrial surfaces was a net emission of 607 [−513; 1653] $Mg \cdot a^{-1}$, although the uncertainty range is considerable. This estimate was 3 times lower than previous estimates.[169,170] In our estimates, surprisingly, Hg-enriched sites (contaminated, naturally enriched, and mining) emitted 217 [202; 258] $Mg \cdot a^{-1}$, which is only about a third of estimated global terrestrial Hg^0 emissions. The emissions estimated from Hg-enriched areas were a much smaller contribution than others have suggested, generally estimating much more than 50% of the total emissions.[31] In our study, this is due to a relatively small area applied to Hg-enriched fluxes. Urban surfaces (e.g., pavements, windows, or roofs) are an insignificant source of global Hg^0 emissions.[35,171] Importantly, Hg^0 emissions from atmospherically influenced areas (i.e., atmospheric Hg^0 levels >3 ng m^{-3}) contributed 261 [114; 359] $Mg \cdot a^{-1}$ of Hg^0 emissions, or about 45% of the total global

DOI: 10.1021/acs.est.5b04013
Environ. Sci. Technol. 2016, 50, 507−524

terrestrial Hg^0 contributions and exceeding emissions for Hg-enriched sites by almost a factor 2. These emissions stem mainly from East Asia (China, Korea, and Japan) and India with high atmospheric Hg^0 levels based on a global atmospheric model,[168] and they indicate the emerging importance of atmospherically impacted areas for atmospheric emissions, or likely re-emission of previous atmospheric deposition, that are currently not included in global estimates.

The largest uncertainty in our estimates, however, is driven by global forests, which in turn is due to a highly uncertain role of foliar surfaces. For example, while the median flux estimate for forest leaves suggested a net deposition of 59 $Mg{\cdot}a^{-1}$, the uncertainty range (37.5th−62.5th percentiles) was from a deposition of 727 $Mg{\cdot}a^{-1}$ to an emission of 703 $Mg{\cdot}a^{-1}$. The median value was lower than estimates by Obrist[172] who calculated global annual leaf total Hg uptake of 237.6 $Mg{\cdot}a^{-1}$. Global foliage provides a well-known Hg^0 sink as observed in many studies, but the current flux data do not provide reliable estimates of the role of plant leaves in global Hg^0 exchanges, adding key uncertainties for Hg budgets. Based on flux data alone, it is even impossible to clearly state if global terrestrial ecosystems serve as net sinks or net sources of atmospheric Hg^0. Other background land covers are better defined in regards to their role as Hg^0 sinks and sources, since direct ecosystem-level fluxes are available. For example, grasslands/shrublands showed a net deposition of 89 [0; 322] $Mg{\cdot}a^{-1}$ and unvegetated areas (i.e., bare soils) showed a net emission of 17 [−1; 51] $Mg{\cdot}a^{-1}$.

The total terrestrial contribution to atmospheric Hg^0 in the contiguous United States was 26 [−42; 88] $Mg{\cdot}a^{-1}$, including 1 [−58; 56] $Mg{\cdot}a^{-1}$ from background sites and 25 [16; 32] $Mg{\cdot}a^{-1}$ from Hg-enriched areas, again with forest flux adding considerable uncertainties. Here, background areas represented 4% of total terrestrial Hg^0 emissions. Hartman et al.[173] estimated, based on a classification and regression tree for three main background land covers in the Unites States (deciduous forest, grassland, and semiarid desert), a net deposition of 8.24 $Mg{\cdot}a^{-1}$, which is in the same order of magnitude as we estimated from these three landscapes (−13 $Mg{\cdot}a^{-1}$). Higher emissions in the United States were proposed by Ericksen et al.[31] with 43 $Mg{\cdot}.a^{-1}$ from background soils, but these did not include vegetation that partially offset such soil emissions. Finally, Hg^0 contributions from atmospherically influenced and Hg-enriched sites were estimated to be 11 [10; 13] $Mg{\cdot}.a^{-1}$ and 13 [6; 19] $Mg{\cdot}a^{-1}$, respectively. Therefore, our estimates of Hg^0 evasion from Hg-enriched areas was in similar range to emissions proposed just for the State of Nevada (10.4 $Mg{\cdot}a^{-1}$)[65] and much lower than previous estimates for the United States of 52 $Mg{\cdot}a^{-1}$ (ranging from 34 to 69 $Mg{\cdot}a^{-1}$).[31] As stated above, the lower emissions estimated in our study were likely due to the relatively small area of Hg-enriched sites in the United States as assessed by a new U.S. Geological Survey data set.[68]

8. SUMMARY

Data compiled for this analysis showed a large under-representation of Hg^0 fluxes from remote background sites and that fluxes were strongly biased geographically (toward measurements in the United States, East-Asia, and Europe) and in time (toward summer and daytime measurements). We observed that among individual studies, the dominant reported controlling factors influencing terrestrial Hg^0 fluxes were solar radiation, soil and air temperatures, and substrate Hg concentrations. Most correlations were lost when all data in the database were included in the correlation analysis. This indicated differing roles of environmental controls among different sites and the presence of strong between-site heterogeneity which overwhelmed differences caused by individual variables, but also may indicate problems and inconsistencies in flux measurements based on different methodologies, and time of measurement. Standardization of measurements is strongly required to obtain comparable data and properly evaluate controlling factors on larger spatial- and temporal-scales.

Atmospheric Hg^0 concentration, however, was negatively correlated with Hg^0 fluxes across background sites, attributed to the presence of Hg^0 flux compensation points. In Hg-enriched sites, Hg^0 fluxes were largely influenced by substrate Hg concentrations promoting Hg^0 emissions, which in turn increased atmospheric Hg^0 concentrations at these sites. Soil covers (plant, litter, and snow) substantially reduced Hg^0 fluxes compared to bare soil.

A worldwide scaling up of Hg^0 fluxes revealed the following patterns:

(1) Background areas contribute Hg^0 emissions in the same order of magnitude as Hg-enriched sites (contaminated, naturally enriched, and mining).
(2) Hg^0 emissions from atmospherically influenced sites (i.e., sites exposed to air concentrations >3 ng m^{-3}), particularly in East Asia, need to be considered as an important global-scale Hg^0 source and contribute the major fraction of Hg^0 emissions to the atmosphere.
(3) Vegetated areas likely constitute an important Hg^0 sink, although reliable vegetation flux measurements, particularly over forests, currently are lacking.
(4) Uncertainties in the role of vegetation are large and likely due to methodological problems in quantifying foliar fluxes; the flux uncertainty of forest foliar measurements could potentially offset any terrestrial Hg^0 emissions, or double current Hg^0 emission estimates, and lead to a shift in the role of global terrestrial ecosystems serving as a net source to a net sink of atmospheric Hg^0.

■ ASSOCIATED CONTENT

Supporting Information

The Supporting Information is available free of charge on the ACS Publications website at DOI: 10.1021/acs.est.5b04013.

Figures (Figure S1 and S2) and table (Table S1), as well as detailed description of Hg^0 flux measurement methodologies (SI 1) and method used for scaling up Hg^0 exchanges (SI 2) (PDF)

■ AUTHOR INFORMATION

Corresponding Authors

*(Y.A.) E-mail: yannick.agnan@biogeochimie.fr.
*(D.O.) Phone: (775) 674-7008; fax: (775) 674-7016; e-mail: daniel.obrist@dri.edu.

Notes

The authors declare no competing financial interest.

■ ACKNOWLEDGMENTS

This project was funded in large parts by the National Science Foundation's (NSF) Coupled-Natural-Human System through Award No. 1313755 to J. Perlinger, N. Selin, S. Wu, D. Obrist,

DOI: 10.1021/acs.est.5b04013
Environ. Sci. Technol. 2016, 50, 507−524

and E. Norman. Partial support was also received through: NSF Award No. 1304305; NASA Experimental Program to Stimulate Competitive Research (EPCoR) Cooperative Agreement Number NNX14AN24A; and internal funding by the Desert Research Institute. We thank Roger Kreidberg for editorial support. Thanks to five anonymous reviewers for their relevant comments which improved this manuscript.

REFERENCES

(1) Horvat, M.; Gibičar, D. Speciation of mercury: Environment, food, clinical, and occupational health. In *Handbook of Elemental Speciation II—Species in the Environment, Food, Medicine and Occupational Health*; R. C, J. C. A, H. C. A, K. H. A, Eds.; John Wiley & Sons, Ltd, 2005; pp 281−304.

(2) Sprovieri, F.; Pirrone, N.; Ebinghaus, R.; Kock, H.; Dommergue, A. A review of worldwide atmospheric mercury measurements. *Atmos. Chem. Phys.* **2010**, *10* (17), 8245−8265.

(3) Steffen, A.; Lehnherr, I.; Cole, A.; Ariya, P.; Dastoor, A.; Durnford, D.; Kirk, J.; Pilote, M. Atmospheric mercury in the Canadian Arctic. Part I: a review of recent field measurements. *Sci. Total Environ.* **2015**, *509−510*, 3−15.

(4) Cole, A. S.; Steffen, A.; Pfaffhuber, K. A.; Berg, T.; Pilote, M.; Poissant, L.; Tordon, R.; Hung, H. Ten-year trends of atmospheric mercury in the high Arctic compared to Canadian sub-Arctic and mid-latitude sites. *Atmos. Chem. Phys.* **2013**, *13* (3), 1535−1545.

(5) Berg, T.; Sekkesæter, S.; Steinnes, E.; Valdal, A.-K.; Wibetoe, G. Springtime depletion of mercury in the European Arctic as observed at Svalbard. *Sci. Total Environ.* **2003**, *304* (1−3), 43−51.

(6) Brooks, S.; Arimoto, R.; Lindberg, S.; Southworth, G. Antarctic polar plateau snow surface conversion of deposited oxidized mercury to gaseous elemental mercury with fractional long-term burial. *Atmos. Environ.* **2008**, *42* (12), 2877−2884.

(7) Brooks, S.; Lindberg, S.; Southworth, G.; Arimoto, R. Springtime atmospheric mercury speciation in the McMurdo, Antarctica coastal region. *Atmos. Environ.* **2008**, *42* (12), 2885−2893.

(8) Angot, H.; Barret, M.; Magand, O.; Ramonet, M.; Dommergue, A. A 2-year record of atmospheric mercury species at a background Southern Hemisphere station on Amsterdam Island. *Atmos. Chem. Phys.* **2014**, *14* (20), 11461−11473.

(9) Slemr, F.; Angot, H.; Dommergue, A.; Magand, O.; Barret, M.; Weigelt, A.; Ebinghaus, R.; Brunke, E.-G.; Pfaffhuber, K. A.; Edwards, G.; et al. Comparison of mercury concentrations measured at several sites in the Southern Hemisphere. *Atmos. Chem. Phys.* **2015**, *15* (6), 3125−3133.

(10) Driscoll, C. T.; Mason, R. P.; Chan, H. M.; Jacob, D. J.; Pirrone, N. Mercury as a global pollutant: sources, pathways, and effects. *Environ. Sci. Technol.* **2013**, *47* (10), 4967−4983.

(11) UNEP. *Global Mercury Assessment 2013: Sources, Emissions, Releases, And Environmental Transport*; UNEP Chemicals Branch: Geneva, Switzerland, 2013.

(12) Selin, N. E.; Jacob, D. J.; Park, R. J.; Yantosca, R. M.; Strode, S.; Jaeglé, L.; Jaffe, D. Chemical cycling and deposition of atmospheric mercury: global constraints from observations. *J. Geophys. Res.* **2007**, *112* (D2).10.1029/2006JD007450

(13) Holmes, C. D.; Jacob, D. J.; Sørensen, A. L.; Corbitt, E. S. Global atmospheric budget of mercury including oxidation of Hg(0) by bromine atoms. *Atmos. Chem. Phys.* **2010**, *74* (12), A413−A413.

(14) Mason, R. P.; Choi, A. L.; Fitzgerald, W. F.; Hammerschmidt, C. R.; Lamborg, C. H.; Soerensen, A. L.; Sunderland, E. M. Mercury biogeochemical cycling in the ocean and policy implications. *Environ. Res.* **2012**, *119*, 101−117.

(15) AMAP/UNEP. *Technical Background Report for the Global Mercury Assessment 2013. Arctic Monitoringand Assessment Programme, Oslo, Norway*; UNEP ChemicalsBranch: Geneva, Switzerland, 2013.

(16) Corbitt, E. S.; Jacob, D. J.; Holmes, C. D.; Streets, D. G.; Sunderland, E. M. Global source-receptor relationships for mercury deposition under present-day and 2050 emissions scenarios. *Environ. Sci. Technol.* **2011**, *45* (24), 10477−10484.

(17) Amos, H. M.; Jacob, D. J.; Streets, D. G.; Sunderland, E. M. Legacy impacts of all-time anthropogenic emissions on the global mercury cycle. *Glob. Biogeochem. Cycles* **2013**, *27* (2), 410−421.

(18) Ericksen, J.; Gustin, M. Foliar exchange of mercury as a function of soil and air mercury concentrations. *Sci. Total Environ.* **2004**, *324* (1−3), 271−279.

(19) Lee, X.; Benoit, G.; Hu, X. Total gaseous mercury concentration and flux over a coastal saltmarsh vegetation in Connecticut, USA. *Atmos. Environ.* **2000**, *34* (24), 4205−4213.

(20) Miller, M. B.; Gustin, M. S.; Eckley, C. S. Measurement and scaling of air−surface mercury exchange from substrates in the vicinity of two Nevada gold mines. *Sci. Total Environ.* **2011**, *409* (19), 3879−3886.

(21) Xiao, Z. F.; Munthe, J.; Schroeder, W. H.; Lindqvist, O. Vertical fluxes of volatile mercury over forest soil and lake surfaces in Sweden. *Tellus B* **1991**, *43* (3), 267−279.

(22) Engle, M. A.; Gustin, M. S.; Zhang, H. Quantifying natural source mercury emissions from the Ivanhoe Mining District, north-central Nevada, USA. *Atmos. Environ.* **2001**, *35* (23), 3987−3997.

(23) Ferrara, R.; Maserti, B. E.; Andersson, M.; Edner, H.; Ragnarson, P.; Svanberg, S.; Hernandez, A. Atmospheric mercury concentrations and fluxes in the Almadén district (Spain). *Atmos. Environ.* **1998**, *32* (22), 3897−3904.

(24) Gustin, M. S.; Taylor, G. E.; Leonard, T. L.; Keislar, R. E. Atmospheric mercury concentrations associated with geologically and anthropogenically enriched sites in central western Nevada. *Environ. Sci. Technol.* **1996**, *30* (8), 2572−2579.

(25) Nacht, D. M.; Gustin, M. S. Mercury emissions from background and altered geologic units throughout Nevada. *Water, Air, Soil Pollut.* **2004**, *151* (1−4), 179−193.

(26) Wang, S.; Feng, X.; Qiu, G.; Wei, Z.; Xiao, T. Mercury emission to atmosphere from Lanmuchang Hg−Tl mining area, Southwestern Guizhou, China. *Atmos. Environ.* **2005**, *39* (39), 7459−7473.

(27) Kim, K.-H.; Lindberg, S. E.; Meyers, T. P. Micrometeorological measurements of mercury vapor fluxes over background forest soils in eastern Tennessee. *Atmos. Environ.* **1995**, *29* (2), 267−282.

(28) Poissant, L.; Casimir, A. Water-air and soil-air exchange rate of total gaseous mercury measured at background sites. *Atmos. Environ.* **1998**, *32* (5), 883−893.

(29) Zhang, H.; Lindberg, S. E.; Marsik, F. J.; Keeler, G. J. Mercury air/surface exchange kinetics of background soils of the Tahquamenon River watershed in the Michigan Upper Peninsula. *Water, Air, Soil Pollut.* **2001**, *126* (1−2), 151−169.

(30) Kuiken, T.; Zhang, H.; Gustin, M.; Lindberg, S. Mercury emission from terrestrial background surfaces in the eastern USA. Part I: Air/surface exchange of mercury within a southeastern deciduous forest (Tennessee) over one year. *Appl. Geochem.* **2008**, *23* (3), 345−355.

(31) Ericksen, J. A.; Gustin, M. S.; Xin, M.; Weisberg, P. J.; Fernandez, G. C. J. Air−soil exchange of mercury from background soils in the United States. *Sci. Total Environ.* **2006**, *366* (2−3), 851−863.

(32) Gustin, M. S.; Taylor, G. E.; Maxey, R. A. Effect of temperature and air movement on the flux of elemental mercury from substrate to the atmosphere. *J. Geophys. Res.* **1997**, *102* (D3), 3891−3898.

(33) Frescholtz, T. F.; Gustin, M. S. Soil and foliar mercury emission as a function of soil concentration. *Water, Air, Soil Pollut.* **2004**, *155* (1−4), 223−237.

(34) Carpi, A.; Lindberg, S. E. Application of a Teflon™ dynamic flux chamber for quantifying soil mercury flux: tests and results over background soil. *Atmos. Environ.* **1998**, *32* (5), 873−882.

(35) Eckley, C. S.; Branfireun, B. Gaseous mercury emissions from urban surfaces: controls and spatiotemporal trends. *Appl. Geochem.* **2008**, *23* (3), 369−383.

(36) Fu, X.; Feng, X.; Zhang, H.; Yu, B.; Chen, L. Mercury emissions from natural surfaces highly impacted by human activities in Guangzhou province, South China. *Atmos. Environ.* **2012**, *54*, 185−193.

DOI: 10.1021/acs.est.5b04013
Environ. Sci. Technol. 2016, 50, 507−524

(37) Lin, C.-J.; Pehkonen, S. O. The chemistry of atmospheric mercury: a review. *Atmos. Environ.* **1999**, *33* (13), 2067−2079.
(38) Almeida, M. D.; Marins, R. V.; Paraquetti, H. H. M.; Bastos, W. R.; Lacerda, L. D. Mercury degassing from forested and open field soils in Rondônia, Western Amazon, Brazil. *Chemosphere* **2009**, *77* (1), 60−66.
(39) Poissant, L.; Pilote, M.; Casimir, A. Mercury flux measurements in a naturally enriched area: correlation with environmental conditions during the Nevada Study and Tests of the Release of Mercury from Soils (STORMS). *J. Geophys. Res.* **1999**, *104* (D17), 21845−21857.
(40) Lindberg, S. E.; Zhang, H.; Gustin, M.; Vette, A.; Marsik, F.; Owens, J.; Casimir, A.; Ebinghaus, R.; Edwards, G.; Fitzgerald, C.; et al. Increases in mercury emissions from desert soils in response to rainfall and irrigation. *J. Geophys. Res.* **1999**, *104* (D17), 21879−21888.
(41) Zhang, H.; Lindberg, S. E.; Kuiken, T. Mysterious diel cycles of mercury emission from soils held in the dark at constant temperature. *Atmos. Environ.* **2008**, *42* (21), 5424−5433.
(42) Wallschläger, D.; Turner, R. R.; London, J.; Ebinghaus, R.; Kock, H. H.; Sommar, J.; Xiao, Z. Factors affecting the measurement of mercury emissions from soils with flux chambers. *J. Geophys. Res.* **1999**, *104* (D17), 21859−21871.
(43) Lindberg, S. E.; Kim, K.-H.; Meyers, T. P.; Owens, J. G. Micrometeorological gradient approach for quantifying air/surface exchange of mercury vapor: tests over contaminated soils. *Environ. Sci. Technol.* **1995**, *29* (1), 126−135.
(44) Gustin, M. S.; Stamenkovic, J. Effect of watering and soil moisture on mercury emissions from soils. *Biogeochemistry* **2005**, *76* (2), 215−232.
(45) Hanson, P. J.; Lindberg, S. E.; Tabberer, T. A.; Owens, J. G.; Kim, K.-H. Foliar exchange of mercury vapor: evidence for a compensation point. *Water, Air, Soil Pollut.* **1995**, *80* (1−4), 373−382.
(46) Zhu, J.; Wang, D.; Liu, X.; Zhang, Y. Mercury fluxes from air/surface interfaces in paddy field and dry land. *Appl. Geochem.* **2011**, *26* (2), 249−255.
(47) Xin, M.; Gustin, M.; Johnson, D. Laboratory investigation of the potential for re-emission of atmospherically derived Hg from soils. *Environ. Sci. Technol.* **2007**, *41* (14), 4946−4951.
(48) Edwards, G. C.; Howard, D. A. Air-surface exchange measurements of gaseous elemental mercury over naturally enriched and background terrestrial landscapes in Australia. *Atmos. Chem. Phys.* **2013**, *13* (10), 5325−5336.
(49) Choi, H.-D.; Holsen, T. M. Gaseous mercury fluxes from the forest floor of the Adirondacks. *Environ. Pollut.* **2009**, *157* (2), 592−600.
(50) Coolbaugh, M.; Gustin, M.; Rytuba, J. Annual emissions of mercury to the atmosphere from natural sources in Nevada and California. *Environ. Geol.* **2002**, *42* (4), 338−349.
(51) Edwards, G. C.; Rasmussen, P. E.; Schroeder, W. H.; Kemp, R. J.; Dias, G. M.; Fitzgerald-Hubble, C. R.; Wong, E. K.; Halfpenny-Mitchell, L.; Gustin, M. S. Sources of variability in mercury flux measurements. *J. Geophys. Res.* **2001**, *106* (D6), 5421−5435.
(52) Ma, M.; Wang, D.; Sun, R.; Shen, Y.; Huang, L. Gaseous mercury emissions from subtropical forested and open field soils in a national nature reserve, southwest China. *Atmos. Environ.* **2013**, *64*, 116−123.
(53) Wang, D.; He, L.; Shi, X.; Wei, S.; Feng, X. Release flux of mercury from different environmental surfaces in Chongqing, China. *Chemosphere* **2006**, *64* (11), 1845−1854.
(54) Eckley, C. S.; Gustin, M.; Marsik, F.; Miller, M. B. Measurement of surface mercury fluxes at active industrial gold mines in Nevada (USA). *Sci. Total Environ.* **2011**, *409* (3), 514−522.
(55) Ferrara, R.; Maserti, B. E.; Andersson, M.; Edner, H.; Ragnarson, P.; Svanberg, S. Mercury degassing rate from mineralized areas in the Mediterranean basin. *Water, Air, Soil Pollut.* **1997**, *93* (1−4), 59−66.
(56) Laurikkala, J.; Juhola, M.; Kentala, E. Informal identification of outliers in medical data. In *Fifth International Workshop on Intelligent Data Analysis in Medicine and Pharmacology IDAMAP-200 Berlin, 22 August. Organized as a workshop of the 14th European Conference on Artificial Intelligence ECAI-2000*; 2000.
(57) Wickham, H. *ggplot2: Elegant Graphics for Data Analysis*, 1st ed.; Springer: Dordrecht, 2009.
(58) Bailey, E. H.; Clark, A. L.; Smith, R. M. Mercury. In *United States Mineral Resources*; Brobst, D. A., Pratt, W. P., Eds.; U.S. Geological Survey, 1973; Vol. *821*, pp 410−414.
(59) Rytuba, J. J. Mercury from mineral deposits and potential environmental impact. *Sci. Total Environ.* **2003**, *43* (3), 326−338.
(60) Gustin, M. S.; Lindberg, S.; Marsik, F.; Casimir, A.; Ebinghaus, R.; Edwards, G.; Hubble-Fitzgerald, C.; Kemp, R.; Kock, H.; Leonard, T.; et al. Nevada STORMS project: measurement of mercury emissions from naturally enriched surfaces. *J. Geophys. Res.* **1999**, *104* (D17), 21831−21844.
(61) Connor, J. J.; Shacklette, H. T.; Ebens, R. J.; Erdman, J. A.; Miesch, A. T.; Tidball, R. R.; Tourtelot, H. A. *Background geochemistry of Some Rocks, Soils, Plants, And Vegetables in the Conterminous United States*, PP-574-F; United States Geological Survey, 1975; p 167.
(62) Mason, B.; Moore, C. B. *Principle of geochemistry*, 4th ed.; Wiley: New York, 1982.
(63) Gustin, M. S.; Lindberg, S. E.; Austin, K.; Coolbaugh, M.; Vette, A.; Zhang, H. Assessing the contribution of natural sources to regional atmospheric mercury budgets. *Sci. Total Environ.* **2000**, *259* (1), 61−71.
(64) Tipping, E.; Lofts, S.; Hooper, H.; Frey, B.; Spurgeon, D.; Svendsen, C. Critical limits for Hg(II) in soils, derived from chronic toxicity data. *Environ. Pollut.* **2010**, *158* (7), 2465−2471.
(65) Zehner, R. E.; Gustin, M. S. Estimation of mercury vapor flux from natural substrate in Nevada. *Environ. Sci. Technol.* **2002**, *36* (19), 4039−4045.
(66) Andersson, A. Mercury in soils. In *The Biogeochemistry of Mercury in the Environment*; Nriagu, J. O., Ed.; Elsevier Biomedical Press: Amsterdam, 1979; pp 79−106.
(67) Lindqvist, O.; Johansson, K.; Bringmark, L.; Timm, B.; Aastrup, M.; Andersson, A.; Hovsenius, G.; Håkanson, L.; Iverfeldt, Å.; Meili, M. Mercury in the Swedish environment — Recent research on causes, consequences and corrective methods. *Water, Air, Soil Pollut.* **1991**, *55* (1−2), xi−261.
(68) Smith, D. B.; Cannon, W. F.; Woodruff, L. G.; Solano, F.; Kilburn, J. E.; Fey, D. L. *Geochemical and Mineralogical Data for Soils of the Conterminous United States*; Data series 801; U.S. Geological Survey, 2013.
(69) Rasmussen, P. E. Current methods of estimating atmospheric mercury fluxes in remote areas. *Environ. Sci. Technol.* **1994**, *28* (13), 2233−2241.
(70) Gustin, M. S.; Rasmussen, P.; Edwards, G.; Schroeder, W.; Kemp, J. Application of a laboratory gas exchange chamber for assessment of in situ mercury emissions. *J. Geophys. Res.* **1999**, *104* (D17), 21873−21878.
(71) Liu, F.; Cheng, H.; Yang, K.; Zhao, C.; Liu, Y.; Peng, M.; Li, K. Characteristics and influencing factors of mercury exchange flux between soil and air in Guangzhou City. *J. Geochem. Explor.* **2014**, *139*, 115−121.
(72) Nacht, D. M.; Gustin, M. S.; Engle, M. A.; Zehner, R. E.; Giglini, A. D. Atmospheric mercury emissions and speciation at the sulphur bank mercury mine superfund site, Northern California. *Environ. Sci. Technol.* **2004**, *38* (7), 1977−1983.
(73) Schroeder, W. H.; Beauchamp, S.; Edwards, G.; Poissant, L.; Rasmussen, P.; Tordon, R.; Dias, G.; Kemp, J.; Van Heyst, B.; Banic, C. M. Gaseous mercury emissions from natural sources in Canadian landscapes. *J. Geophys. Res.* **2005**, *110* (D18), D18302.
(74) Sigler, J. M.; Lee, X. Gaseous mercury in background forest soil in the northeastern United States. *J. Geophys. Res.* **2006**, *111* (G02007).10.1029/2005JG000106
(75) Sommar, J.; Zhu, W.; Shang, L.; Feng, X.; Lin, C.-J. A whole-air relaxed eddy accumulation measurement system for sampling vertical vapour exchange of elemental mercury. *Tellus, Ser. B* **2013**, *65* (19940).10.3402/tellusb.v65i0.19940

DOI: 10.1021/acs.est.5b04013
Environ. Sci. Technol. 2016, 50, 507−524

(76) Aubin, I.; Beaudet, M.; Messier, C. Light extinction coefficients specific to the understory vegetation of the southern boreal forest, Quebec. *Can. J. For. Res.* **2000**, *30* (1), 168−177.
(77) Leigh, E. G. Structure and climate in tropical rain forest. *Annu. Rev. Ecol. Syst.* **1975**, *6*, 67−86.
(78) Lowman, M. D.; Rinker, H. B. *Forest Canopies*, 2 ed.; Academic Press: Amsterdam, 2004.
(79) Obrist, D.; Pearson, C.; Webster, J.; Kane, T.; Lin, J.; Aiken, G. A.; Alpers, C. N. Terrestrial mercury in the western United States: aboveground biomass and soil Hg concentrations and distributions. *Sci. Total Environ.*, in press (http://dx.doi.org/10.1016/j.scitotenv.2015.11.104).
(80) Lindberg, S. E.; Jackson, D. R.; Huckabee, J. W.; Jansen, S. A.; Levin, M. J.; Lund, J. R. Atmospheric emission and plant uptake of mercury from agricultural soils near the Almadén mercury mine. *J. Environ. Qual.* **1979**, *8* (4), 572−578.
(81) Gustin, M. S.; Ericksen, J. A.; Schorran, D. E.; Johnson, D. W.; Lindberg, S. E.; Coleman, J. S. Application of controlled mesocosms for understanding mercury air-soil-plant exchange. *Environ. Sci. Technol.* **2004**, *38* (22), 6044−6050.
(82) Kuiken, T.; Gustin, M.; Zhang, H.; Lindberg, S.; Sedinger, B. Mercury emission from terrestrial background surfaces in the eastern USA. II: Air/surface exchange of mercury within forests from South Carolina to New England. *Appl. Geochem.* **2008**, *23* (3), 356−368.
(83) Ericksen, J. A.; Gustin, M. S.; Schorran, D. E.; Johnson, D. W.; Lindberg, S. E.; Coleman, J. S. Accumulation of atmospheric mercury in forest foliage. *Atmos. Environ.* **2003**, *37* (12), 1613−1622.
(84) Gustin, M. S. Exchange of mercury between the atmosphere and terrestrial ecosystems. In *Environmental Chemistry and Toxicology of Mercury*; Liu, G., Cai, Y., O'Driscoll, N., Eds.; John Wiley & Sons, Inc., 2011; pp 423−451.
(85) Rutter, A. P.; Schauer, J. J.; Shafer, M. M.; Creswell, J. E.; Olson, M. R.; Robinson, M.; Collins, R. M.; Parman, A. M.; Katzman, T. L.; Mallek, J. L. Dry deposition of gaseous elemental mercury to plants and soils using mercury stable isotopes in a controlled environment. *Atmos. Environ.* **2011**, *45* (4), 848−855.
(86) Frescholtz, T. F.; Gustin, M. S.; Schorran, D. E.; Fernandez, G. C. J. Assessing the source of mercury in foliar tissue of quaking aspen. *Environ. Toxicol. Chem.* **2003**, *22* (9), 2114−2119.
(87) Millhollen, A. G.; Gustin, M. S.; Obrist, D. Foliar mercury accumulation and exchange for three tree species. *Environ. Sci. Technol.* **2006**, *40* (19), 6001−6006.
(88) Munthe, J.; Hultberg, H.; Iverfeldt, Å. Mechanisms of deposition of methylmercury and mercury to coniferous forests. *Water, Air, Soil Pollut.* **1995**, *80* (1−4), 363−371.
(89) St. Louis, V. L.; Rudd, J. W. M.; Kelly, C. A.; Hall, B. D.; Rolfhus, K. R.; Scott, K. J.; Lindberg, S. E.; Dong, W. Importance of the forest canopy to fluxes of methyl mercury and total mercury to boreal ecosystems. *Environ. Sci. Technol.* **2001**, *35* (15), 3089−3098.
(90) Grigal, D. F.; Kolka, R. K.; Fleck, J. A.; Nater, E. A. Mercury budget of an upland-peatland watershed. *Biogeochemistry* **2000**, *50* (1), 95−109.
(91) Bishop, K. H.; Lee, Y.-H. Catchments as a source of mercury/methylmercury in boreal surface waters. In *Metal Ions in Biological Systems. Vol. 34: Mercury and Its Effects on Environment and Biology*; Sigel, A., Sigel, H., Eds.; Marcel Dekker: New York, 1997; pp 113−130.
(92) Rea, A. W.; Keeler, G. J.; Scherbatskoy, T. The deposition of mercury in throughfall and litterfall in the lake champlain watershed: a short-term study. *Atmos. Environ.* **1996**, *30* (19), 3257−3263.
(93) Jiskra, M.; Wiederhold, J. G.; Skyllberg, U.; Kronberg, R.-M.; Hajdas, I.; Kretzschmar, R. Mercury deposition and re-emission pathways in boreal forest soils investigated with Hg isotope signatures. *Environ. Sci. Technol.* **2015**, *49* (12), 7188−7196.
(94) Demers, J. D.; Blum, J. D.; Zak, D. R. Mercury isotopes in a forested ecosystem: implications for air-surface exchange dynamics and the global mercury cycle. *Glob. Biogeochem. Cycles* **2013**, *27* (1), 222−238.
(95) Stamenkovic, J.; Gustin, M. S.; Arnone, J. A., III; Johnson, D. W.; Larsen, J. D.; Verburg, P. S. J. Atmospheric mercury exchange with a tallgrass prairie ecosystem housed in mesocosms. *Sci. Total Environ.* **2008**, *406* (1−2), 227−238.
(96) Asner, G. P.; Scurlock, J. M.; A Hicke, J. Global synthesis of leaf area index observations: implications for ecological and remote sensing studies. *Glob. Ecol. Biogeogr.* **2003**, *12* (3), 191−205.
(97) Blackwell, B. D.; Driscoll, C. T.; Maxwell, J. A.; Holsen, T. M. Changing climate alters inputs and pathways of mercury deposition to forested ecosystems. *Biogeochemistry* **2014**, *119* (1−3), 215−228.
(98) Laacouri, A.; Nater, E. A.; Kolka, R. K. Distribution and uptake dynamics of mercury in leaves of common deciduous tree species in Minnesota, U.S.A. *Environ. Sci. Technol.* **2013**, *47* (18), 10462−10470.
(99) Obrist, D.; Johnson, D. W.; Edmonds, R. L. Effects of vegetation type on mercury concentrations and pools in two adjacent coniferous and deciduous forests. *J. Plant Nutr. Soil Sci.* **2012**, *175* (1), 68−77.
(100) Demers, J. D.; Driscoll, C. T.; Fahey, T. J.; Yavitt, J. B. Mercury cycling in litter and soil in different forest types in the Adirondack region, New York, USA. *Ecol. Appl.* **2007**, *17* (5), 1341−1351.
(101) Nelson, S. J.; Johnson, K. B.; Kahl, J. S.; Haines, T. A.; Fernandez, I. J. Mass balances of mercury and nitrogen in burned and unburned forested watersheds at Acadia National Park, Maine, USA. *Environ. Monit. Assess.* **2007**, *126* (1−3), 69−80.
(102) Poulain, A. J.; Roy, V.; Amyot, M. Influence of temperate mixed and deciduous tree covers on Hg concentrations and photoredox transformations in snow. *Geochim. Cosmochim. Acta* **2007**, *71* (10), 2448−2462.
(103) Witt, E. L.; Kolka, R. K.; Nater, E. A.; Wickman, T. R. Influence of the forest canopy on total and methyl mercury deposition in the boreal forest. *Water, Air, Soil Pollut.* **2009**, *199* (1−4), 3−11.
(104) Medlyn, B. E.; Barton, C. V. M; Broadmeadow, M. S. J.; Ceulemans, R.; De Angelis, P.; Forstreuter, M.; Freeman, M.; Jackson, S. B.; Kellomäki, S.; Laitat, E.; et al. Stomatal conductance of forest species after long-term exposure to elevated CO2 concentration: a synthesis. *New Phytol.* **2001**, *149* (2), 247−264.
(105) Catovsky, S.; Holbrook, N. M.; Bazzaz, F. A. Coupling whole-tree transpiration and canopy photosynthesis in coniferous and broad-leaved tree species. *Can. J. For. Res.* **2002**, *32* (2), 295−309.
(106) Pokharel, A. K.; Obrist, D. Fate of mercury in tree litter during decomposition. *Biogeosciences* **2011**, *8* (9), 2507−2521.
(107) Graydon, J. A.; St. Louis, V. L.; Hintelmann, H.; Lindberg, S. E.; Sandilands, K. A.; Rudd, J. W. M.; Kelly, C. A.; Tate, M. T.; Krabbenhoft, D. P.; Lehnherr, I. Investigation of uptake and retention of atmospheric Hg(II) by boreal forest plants using stable Hg isotopes. *Environ. Sci. Technol.* **2009**, *43* (13), 4960−4966.
(108) Ericksen, J. A.; Gustin, M. S.; Lindberg, S. E.; Olund, S. D.; Krabbenhoft, D. P. Assessing the potential for re-emission of mercury deposited in precipitation from arid soils using a stable isotope. *Environ. Sci. Technol.* **2005**, *39* (20), 8001−8007.
(109) Hintelmann, H.; Harris, R.; Heyes, A.; Hurley, J. P.; Kelly, C. A.; Krabbenhoft, D. P.; Lindberg, S.; Rudd, J. W. M.; Scott, K. J., St; Louis, V. L. Reactivity and mobility of new and old mercury deposition in a boreal forest ecosystem during the first year of the METAALICUS study. *Environ. Sci. Technol.* **2002**, *36* (23), 5034−5040.
(110) Carpi, A.; Lindberg, S. E. Sunlight-mediated emission of elemental mercury from soil amended with municipal sewage sludge. *Environ. Sci. Technol.* **1997**, *31* (7), 2085−2091.
(111) Boudala, F. S.; Folkins, I.; Beauchamp, S.; Tordon, R.; Neima, J.; Johnson, B. Mercury flux measurements over air and water in Kejimkujik National Park, Nova Scotia. *Water, Air, Soil Pollut.* **2000**, *122* (1−2), 183−202.
(112) Obrist, D.; Pokharel, A. K.; Moore, C. Vertical profile measurements of soil air suggest immobilization of gaseous elemental mercury in mineral soil. *Environ. Sci. Technol.* **2014**, *48* (4), 2242−2252.
(113) Faïn, X.; Grangeon, S.; Bahlmann, E.; Fritsche, J.; Obrist, D.; Dommergue, A.; Ferrari, C. P.; Cairns, W.; Ebinghaus, R.; Barbante, C.; et al. Diurnal production of gaseous mercury in the alpine

DOI: 10.1021/acs.est.5b04013
Environ. Sci. Technol. 2016, 50, 507−524

snowpack before snowmelt. *J. Geophys. Res.* **2007**, *112* (D21311).10.1029/2007JD008520
(114) Poulain, A. J.; Lalonde, J. D.; Amyot, M.; Shead, J. A.; Raofie, F.; Ariya, P. A. Redox transformations of mercury in an Arctic snowpack at springtime. *Atmos. Environ.* **2004**, *38* (39), 6763−6774.
(115) Moore, C.; Carpi, A. Mechanisms of the emission of mercury from soil: role of UV radiation. *J. Geophys. Res.* **2005**, *110* (D24302).10.1029/2004JD005567
(116) Lalonde, J. D.; Poulain, A. J.; Amyot, M. The role of mercury redox reactions in snow on snow-to-air mercury transfer. *Environ. Sci. Technol.* **2002**, *36* (2), 174−178.
(117) Amyot, M.; Lean, D.; Mierle, G. Photochemical formation of volatile mercury in high Arctic lakes. *Environ. Toxicol. Chem.* **1997**, *16* (10), 2054−2063.
(118) Amyot, M.; McQueen, D. J.; Mierle, G.; Lean, D. R. S. Sunlight-induced formation of dissolved gaseous mercury in lake waters. *Environ. Sci. Technol.* **1994**, *28* (13), 2366−2371.
(119) Zhang, H.; Lindberg, S. E. Processes influencing the emission of mercury from soils: a conceptual model. *J. Geophys. Res.* **1999**, *104* (D17), 21889−21896.
(120) Alberts, J. J.; Schindler, J. E.; Miller, R. W.; Nutter, D. E. Elemental mercury evolution mediated by humic acid. *Science* **1974**, *184* (4139), 895−897.
(121) Allard, B.; Arsenie, I. Abiotic reduction of mercury by humic substances in aquatic system — an important process for the mercury cycle. *Water, Air, Soil Pollut.* **1991**, *56* (1), 457−464.
(122) Lin, C.; Pehkonen, S. O. Aqueous free radical chemistry of mercury in the presence of iron oxides and ambient aerosol. *Atmos. Environ.* **1997**, *31* (24), 4125−4137.
(123) Barkay, T.; Liebert, C.; Gillman, M. Environmental significance of the potential for mer(Tn21)-mediated reduction of Hg2+ to Hg0 in natural waters. *Appl. Environ. Microbiol.* **1989**, *55* (5), 1196−1202.
(124) Mason, R. P.; Morel, F. M. M.; Hemond, H. F. The role of microorganisms in elemental mercury formation in natural waters. In *Mercury as a Global Pollutant*; Porcella, D. B., Huckabee, J. W., Wheatley, B., Eds.; Springer: Netherlands, 1995; pp 775−787.
(125) Schaefer, J. K.; Letowski, J.; Barkay, T. mer-mediated resistance and volatilization of Hg(II) under anaerobic conditions. *Geomicrobiol. J.* **2002**, *19* (1), 87−102.
(126) Siciliano, S. D.; O'Driscoll, N. J.; Lean, D. R. S. Microbial reduction and oxidation of mercury in freshwater lakes. *Environ. Sci. Technol.* **2002**, *36* (14), 3064−3068.
(127) Rolfhus, K. R.; Fitzgerald, W. F. Mechanisms and temporal variability of dissolved gaseous mercury production in coastal seawater. *Mar. Chem.* **2004**, *90* (1−4), 125−136.
(128) Poulain, A. J.; Amyot, M.; Findlay, D.; Telor, S.; Barkay, T.; Hintelmann, H. Biological and photochemical production of dissolved gaseous mercury in a boreal lake. *Limnol. Oceanogr.* **2004**, *49* (6), 2265−2275.
(129) Fritsche, J.; Obrist, D.; Alewell, C. Evidence of microbial control of Hg0 emissions from uncontaminated terrestrial soils. *J. Plant Nutr. Soil Sci.* **2008**, *171* (2), 200−209.
(130) Voroney, R. P.; Heck, R. J. Soil habitat. In *Soil Microbiology, Ecology and Biochemistry*; Paul, E. A., Ed.; Academic Press: London, UK, 2015; pp 15−39.
(131) Bash, J. O.; Miller, D. R. Growing season total gaseous mercury (TGM) flux measurements over an Acer rubrum L. stand. *Atmos. Environ.* **2009**, *43* (37), 5953−5961.
(132) Poissant, L.; Pilote, M.; Constant, P.; Beauvais, C.; Zhang, H. H.; Xu, X. Mercury gas exchanges over selected bare soil and flooded sites in the bay St. François wetlands (Québec, Canada). *Atmos. Environ.* **2004**, *38* (25), 4205−4214.
(133) Gustin, M. S.; Engle, M.; Ericksen, J.; Lyman, S.; Stamenkovic, J.; Xin, M. Mercury exchange between the atmosphere and low mercury containing substrates. *Appl. Geochem.* **2006**, *21* (11), 1913−1923.
(134) Fritsche, J.; Wohlfahrt, G.; Ammann, C.; Zeeman, M.; Hammerle, A.; Obrist, D.; Alewell, C. Summertime elemental mercury exchange of temperate grasslands on an ecosystem-scale. *Atmos. Chem. Phys.* **2008**, *8* (24), 7709−7722.
(135) Mazur, M.; Mitchell, C. P. J.; Eckley, C. S.; Eggert, S. L.; Kolka, R. K.; Sebestyen, S. D.; Swain, E. B. Gaseous mercury fluxes from forest soils in response to forest harvesting intensity: a field manipulation experiment. *Sci. Total Environ.* **2014**, *496*, 678−687.
(136) Xin, M.; Gustin, M. S. Gaseous elemental mercury exchange with low mercury containing soils: investigation of controlling factors. *Appl. Geochem.* **2007**, *22* (7), 1451−1466.
(137) Graydon, J. A.; St. Louis, V. L.; Lindberg, S. E.; Hintelmann, H.; Krabbenhoft, D. P. Investigation of mercury exchange between forest canopy vegetation and the atmosphere using a new dynamic chamber. *Environ. Sci. Technol.* **2006**, *40* (15), 4680−4688.
(138) Poissant, L.; Pilote, M.; Yumvihoze, E.; Lean, D. Mercury concentrations and foliage/atmosphere fluxes in a maple forest ecosystem in Québec, Canada. *J. Geophys. Res.* **2008**, *113* (D10307).10.1029/2007JD009510
(139) Gabriel, M. C.; Williamson, D. G. Principal biogeochemical factors affecting the speciation and transport of mercury through the terrestrial environment. *Environ. Geochem. Health* **2004**, *26* (3−4), 421−434.
(140) Semu, E.; Singh, B. R.; Selmer-Olsen, A. R. Adsorption of mercury compounds by tropical soils. *Water, Air, Soil Pollut.* **1986**, *27* (1−2), 19−27.
(141) Barrow, N. J.; Cox, V. C. The effects of pH and chloride concentration on mercury sorption. II. By a soil. *J. Soil Sci.* **1992**, *43* (2), 305−312.
(142) Schuster, E. The behavior of mercury in the soil with special emphasis on complexation and adsorption processes - A review of the literature. *Water, Air, Soil Pollut.* **1991**, *56* (1), 667−680.
(143) Meili, M. The coupling of mercury and organic matter in the biogeochemical cycle — towards a mechanistic model for the boreal forest zone. *Water, Air, Soil Pollut.* **1991**, *56* (1), 333−347.
(144) Yin, Y.; Allen, H. E.; Li, Y.; Huang, C. P.; Sanders, P. F. Adsorption of mercury(II) by soil: effects of pH, chloride, and organic matter. *J. Environ. Qual.* **1996**, *25* (4), 837.
(145) Obrist, D.; Faïn, X.; Berger, C. Gaseous elemental mercury emissions and CO2 respiration rates in terrestrial soils under controlled aerobic and anaerobic laboratory conditions. *Sci. Total Environ.* **2010**, *408* (7), 1691−1700.
(146) Fuentes, J. P.; Bezdicek, D. F.; Flury, M.; Albrecht, S.; Smith, J. L. Microbial activity affected by lime in a long-term no-till soil. *Soil Tillage Res.* **2006**, *88* (1−2), 123−131.
(147) Rousk, J.; Bååth, E.; Brookes, P. C.; Lauber, C. L.; Lozupone, C.; Caporaso, J. G.; Knight, R.; Fierer, N. Soil bacterial and fungal communities across a pH gradient in an arable soil. *ISME J.* **2010**, *4* (10), 1340−1351.
(148) Andersson, S.; Nilsson, S. I. Influence of pH and temperature on microbial activity, substrate availability of soil-solution bacteria and leaching of dissolved organic carbon in a mor humus. *Soil Biol. Biochem.* **2001**, *33* (9), 1181−1191.
(149) Bahlmann, E.; Ebinghaus, R.; Ruck, W. Development and application of a laboratory flux measurement system (LFMS) for the investigation of the kinetics of mercury emissions from soils. *J. Environ. Manage.* **2006**, *81* (2), 114−125.
(150) Rinklebe, J.; During, A.; Overesch, M.; Du Laing, G.; Wennrich, R.; Stärk, H.-J.; Mothes, S. Dynamics of mercury fluxes and their controlling factors in large Hg-polluted floodplain areas. *Environ. Pollut.* **2010**, *158* (1), 308−318.
(151) Schroeder, W. H.; Munthe, J.; Lindqvist, O. Cycling of mercury between water, air, and soil compartments of the environment. *Water, Air, Soil Pollut.* **1989**, *48* (3−4), 337−347.
(152) Kim, K.-H.; Lindberg, S. E. Design and initial tests of a dynamic enclosure chamber for measurements of vapor-phase mercury fluxes over soils. *Water, Air, Soil Pollut.* **1995**, *80* (1−4), 1059−1068.
(153) Kim, K. H.; Lindberg, S. E.; Hanson, P. J.; Owens, J.; Myers, T. P. Micrometeorological methods for measurements of mercury emissions over contaminated soils; Oak Ridge National Laboratory, 1993; pp 411−414.

DOI: 10.1021/acs.est.5b04013
Environ. Sci. Technol. 2016, 50, 507−524

(154) Eckley, C. S.; Gustin, M.; Lin, C.-J.; Li, X.; Miller, M. B. The influence of dynamic chamber design and operating parameters on calculated surface-to-air mercury fluxes. *Atmos. Environ.* **2010**, *44* (2), 194−203.
(155) Zhu, W.; Sommar, J.; Lin, C.-J.; Feng, X. Mercury vapor air−surface exchange measured by collocated micrometeorological and enclosure methods − Part I: Data comparability and method characteristics. *Atmos. Chem. Phys.* **2015**, *15* (2), 685−702.
(156) Gustin, M. S.; Lindberg, S. E. Assessing the contribution of natural sources to the global mercury cycle: the importance of intercomparing dynamic flux measurements. *Fresenius' J. Anal. Chem.* **2000**, *366* (5), 417−422.
(157) Lindberg, S. E.; Zhang, H.; Vette, A. F.; Gustin, M. S.; Barnett, M. O.; Kuiken, T. Dynamic flux chamber measurement of gaseous mercury emission fluxes over soils. Part 2: effect of flushing flow rate and verification of a two-resistance exchange interface simulation model. *Atmos. Environ.* **2002**, *36* (5), 847−859.
(158) Carpi, A.; Frei, A.; Cocris, D.; McCloskey, R.; Contreras, E.; Ferguson, K. Analytical artifacts produced by a polycarbonate chamber compared to a Teflon chamber for measuring surface mercury fluxes. *Anal. Bioanal. Chem.* **2007**, *388* (2), 361−365.
(159) Gillis, A.; Miller, D. R. Some potential errors in the measurement of mercury gas exchange at the soil surface using a dynamic flux chamber. *Sci. Total Environ.* **2000**, *260* (1), 181−189.
(160) Zhang, H.; Lindberg, S. E.; Barnett, M. O.; Vette, A. F.; Gustin, M. S. Dynamic flux chamber measurement of gaseous mercury emission fluxes over soils. Part 1: simulation of gaseous mercury emissions from soils using a two-resistance exchange interface model. *Atmos. Environ.* **2002**, *36* (5), 835−846.
(161) Engle, M. A.; Gustin, M. S.; Goff, F.; Counce, D. A.; Janik, C. J.; Bergfeld, D.; Rytuba, J. J. Atmospheric mercury emissions from substrates and fumaroles associated with three hydrothermal systems in the western United States. *J. Geophys. Res.* **2006**, *111* (D17), D17304.
(162) Selin, N. E.; Jacob, D. J.; Yantosca, R. M.; Strode, S.; Jaeglé, L.; Sunderland, E. M. Global 3-D land-ocean-atmosphere model for mercury: present-day versus preindustrial cycles and anthropogenic enrichment factors for deposition. *Glob. Biogeochem. Cycles* **2008**, *22* (GB2011).n/a10.1029/2007GB003040
(163) Smith-Downey, N. V.; Sunderland, E. M.; Jacob, D. J. Anthropogenic impacts on global storage and emissions of mercury from terrestrial soils: Insights from a new global model. *J. Geophys. Res.* **2010**, *115* (G3), G03008.
(164) Denkenberger, J. S.; Driscoll, C. T.; Branfireun, B. A.; Eckley, C. S.; Cohen, M.; Selvendiran, P. A synthesis of rates and controls on elemental mercury evasion in the Great Lakes Basin. *Environ. Pollut.* **2012**, *161*, 291−298.
(165) Broxton, P. D.; Zeng, X.; Sulla-Menashe, D.; Troch, P. A. A global land cover climatology using MODIS data. *J. Appl. Meteorol. Climatol.* **2014**, *53* (6), 1593−1605.
(166) Latham, J.; Cumani, R.; Rosati, I.; Bloise, M. *Global Land Cover SHARE (GLC-SHARE) database Beta-Release Version 1.0−2014*; FAO, 2014.
(167) Loveland, T. R.; Reed, B. C.; Brown, J. F.; Ohlen, D. O.; Zhu, Z.; Yang, L.; Merchant, J. W. Development of a global land cover characteristics database and IGBP DISCover from 1 km AVHRR data. *Int. J. Remote Sens.* **2000**, *21* (6−7), 1303−1330.
(168) Lei, H.; Liang, X.-Z.; Wuebbles, D. J.; Tao, Z. Model analyses of atmospheric mercury: present air quality and effects of transpacific transport on the United States. *Atmos. Chem. Phys.* **2013**, *13* (21), 10807−10825.
(169) Pirrone, N.; Cinnirella, S.; Feng, X.; Finkelman, R. B.; Friedli, H. R.; Leaner, J.; Mason, R.; Mukherjee, A. B.; Stracher, G. B.; Streets, D. G.; et al. Global mercury emissions to the atmosphere from anthropogenic and natural sources. *Atmos. Chem. Phys.* **2010**, *10* (13), 5951−5964.
(170) Mason, R. Mercury emissions from natural processes and their importance in the global mercury cycle. In *Mercury Fate and Transport in the Global Atmosphere*; Mason, R., Pirrone, N., Eds.; Springer: New York, 2009; pp 173−191.
(171) Gabriel, M. C.; Williamson, D. G.; Zhang, H.; Brooks, S.; Lindberg, S. Diurnal and seasonal trends in total gaseous mercury flux from three urban ground surfaces. *Atmos. Environ.* **2006**, *40* (23), 4269−4284.
(172) Obrist, D. Atmospheric mercury pollution due to losses of terrestrial carbon pools? *Biogeochemistry* **2007**, *85* (2), 119−123.
(173) Hartman, J. S.; Weisberg, P. J.; Pillai, R.; Ericksen, J. A.; Kuiken, T.; Lindberg, S. E.; Zhang, H.; Rytuba, J. J.; Gustin, M. S. Application of a rule-based model to estimate mercury exchange for three background biomes in the continental United States. *Environ. Sci. Technol.* **2009**, *43* (13), 4989−4994.
(174) Baya, A. P.; Van Heyst, B. Assessing the trends and effects of environmental parameters on the behaviour of mercury in the lower atmosphere over cropped land over four seasons. *Atmos. Chem. Phys.* **2010**, *10* (17), 8617−8628.
(175) Brooks, S. B.; Saiz-Lopez, A.; Skov, H.; Lindberg, S. E.; Plane, J. M. C.; Goodsite, M. E. The mass balance of mercury in the springtime arctic environment. *Geophys. Res. Lett.* **2006**, *33* (L13812).10.1029/2005GL025525
(176) Cannon, K.; Dudas, M. J. Seasonal pattern of gaseous mercury emanations from forested soils in Alberta. *Can. J. Soil Sci.* **1982**, *62* (3), 541−543.
(177) Carpi, A.; Fostier, A. H.; Orta, O. R.; dos Santos, J. C.; Gittings, M. Gaseous mercury emissions from soil following forest loss and land use changes: field experiments in the United States and Brazil. *Atmos. Environ.* **2014**, *96*, 423−429.
(178) Cobbett, F. D.; Steffen, A.; Lawson, G.; Van Heyst, B. J. GEM fluxes and atmospheric mercury concentrations (GEM, RGM and Hgp) in the Canadian Arctic at Alert, Nunavut, Canada (February−June 2005). *Atmos. Environ.* **2007**, *41* (31), 6527−6543.
(179) Cobos, D. R.; Baker, J. M.; Nater, E. A. Conditional sampling for measuring mercury vapor fluxes. *Atmos. Environ.* **2002**, *36* (27), 4309−4321.
(180) Converse, A. D.; Riscassi, A. L.; Scanlon, T. M. Seasonal variability in gaseous mercury fluxes measured in a high-elevation meadow. *Atmos. Environ.* **2010**, *44* (18), 2176−2185.
(181) Ferrari, C. P.; Gauchard, P.-A.; Aspmo, K.; Dommergue, A.; Magand, O.; Bahlmann, E.; Nagorski, S.; Temme, C.; Ebinghaus, R.; Steffen, A.; et al. Snow-to-air exchanges of mercury in an Arctic seasonal snow pack in Ny-Ålesund, Svalbard. *Atmos. Environ.* **2005**, *39* (39), 7633−7645.
(182) Fritsche, J.; Obrist, D.; Zeeman, M. J.; Conen, F.; Eugster, W.; Alewell, C. Elemental mercury fluxes over a sub-alpine grassland determined with two micrometeorological methods. *Atmos. Environ.* **2008**, *42* (13), 2922−2933.
(183) Fu, X.; Feng, X.; Wang, S. Exchange fluxes of Hg between surfaces and atmosphere in the eastern flank of Mount Gongga, Sichuan province, southwestern China. *J. Geophys. Res.* **2008**, *113* (D20), D20306.
(184) Kozuchowski, J.; Johnson, D. L. Gaseous emissions of mercury from an aquatic vascular plant. *Nature* **1978**, *274* (5670), 468−469.
(185) Kyllönen, K.; Hakola, H.; Hellén, H.; Korhonen, M.; Verta, M. Atmospheric mercury fluxes in a Southern boreal forest and wetland. *Water, Air, Soil Pollut.* **2012**, *223* (3), 1171−1182.
(186) Lindberg, S. E.; Hanson, P. J.; Meyers, T. P.; Kim, K.-H. Air/surface exchange of mercury vapor over forests—the need for a reassessment of continental biogenic emissions. *Atmos. Environ.* **1998**, *32* (5), 895−908.
(187) Lindberg, S. E.; Dong, W.; Meyers, T. Transpiration of gaseous elemental mercury through vegetation in a subtropical wetland in Florida. *Atmos. Environ.* **2002**, *36* (33), 5207−5219.
(188) Magarelli, G.; Fostier, A. H. Influence of deforestation on the mercury air/soil exchange in the Negro River Basin, Amazon. *Atmos. Environ.* **2005**, *39* (39), 7518−7528.
(189) Obrist, D.; Gustin, M. S.; Arnone, J. A.; Johnson, D. W.; Schorran, D. E.; Verburg, P. S. J. Measurements of gaseous elemental

DOI: 10.1021/acs.est.5b04013
Environ. Sci. Technol. 2016, 50, 507−524

mercury fluxes over intact tallgrass prairie monoliths during one full year. *Atmos. Environ.* **2005**, *39* (5), 957−965.
(190) Obrist, D.; Conen, F.; Vogt, R.; Siegwolf, R.; Alewell, C. Estimation of Hg0 exchange between ecosystems and the atmosphere using 222Rn and Hg0 concentration changes in the stable nocturnal boundary layer. *Atmos. Environ.* **2006**, *40* (5), 856−866.
(191) Olofsson, M.; Sommar, J.; Ljungström, E.; Andersson, M.; Wängberg, I. Application of relaxed eddy accumulation technique to quantify Hg0 fluxes over modified soil surfaces. *Water, Air, Soil Pollut.* **2005**, *167* (1−4), 331−352.
(192) Slemr, F.; Brunke, E.-G.; Whittlestone, S.; Zahorowski, W.; Ebinghaus, R.; Kock, H. H.; Labuschagne, C. 222Rn-calibrated mercury fluxes from terrestrial surface of southern Africa. *Atmos. Chem. Phys.* **2013**, *13* (13), 6421−6428.
(193) Steen, A. O.; Berg, T.; Dastoor, A. P.; Durnford, D. A.; Hole, L. R.; Pfaffhuber, K. A. Dynamic exchange of gaseous elemental mercury during polar night and day. *Atmos. Environ.* **2009**, *43* (35), 5604−5610.
(194) Zhang, H. H.; Poissant, L.; Xu, X.; Pilote, M. Explorative and innovative dynamic flux bag method development and testing for mercury air−vegetation gas exchange fluxes. *Atmos. Environ.* **2005**, *39* (39), 7481−7493.
(195) Fu, X.; Feng, X.; Zhu, W.; Rothenberg, S.; Yao, H.; Zhang, H. Elevated atmospheric deposition and dynamics of mercury in a remote upland forest of southwestern China. *Environ. Pollut.* **2010**, *158* (6), 2324−2333.
(196) Kim, K.-H.; Kim, M.-Y.; Kim, J.; Lee, G. Effects of changes in environmental conditions on atmospheric mercury exchange: comparative analysis from a rice paddy field during the two spring periods of 2001 and 2002. *J. Geophys. Res.* **2003**, *108* (D19).10.1029/2003JD003375
(197) Cobbett, F.; Van Heyst, B. Measurements of GEM fluxes and atmospheric mercury concentrations (GEM, RGM and Hgp) from an agricultural field amended with biosolids in Southern Ont., Canada (October 2004−November 2004). *Atmos. Environ.* **2007**, *41* (11), 2270−2282.
(198) Gabriel, M. C.; Williamson, D. Some insight into the influence of urban ground surface properties on the air-surface exchange of total gaseous mercury. *Appl. Geochem.* **2008**, *23* (4), 794−806.
(199) Gabriel, M. C.; Williamson, D. G.; Brooks, S. Potential impact of rainfall on the air-surface exchange of total gaseous mercury from two common urban ground surfaces. *Atmos. Environ.* **2011**, *45* (9), 1766−1774.
(200) Goodrow, S. M.; Miskewitz, R.; Hires, R. I.; Eisenreich, S. J.; Douglas, W. S.; Reinfelder, J. R. Mercury emissions from cement-stabilized dredged material. *Environ. Sci. Technol.* **2005**, *39* (21), 8185−8190.
(201) Kim, K.-H.; Kim, M.-Y. The exchange of gaseous mercury across soil−air interface in a residential area of Seoul, Korea. *Atmos. Environ.* **1999**, *33* (19), 3153−3165.
(202) Kim, K.-H.; Kim, M.-Y.; Lee, G. The soil−air exchange characteristics of total gaseous mercury from a large-scale municipal landfill area. *Atmos. Environ.* **2001**, *35* (20), 3475−3493.
(203) Kotnik, J.; Horvat, M.; Dizdarevic, T. Current and past mercury distribution in air over the Idrija Hg mine region, Slovenia. *Atmos. Environ.* **2005**, *39* (39), 7570−7579.
(204) Leonard, T. L.; Taylor, G. E.; Gustin, M. S.; Fernandez, G. C. Mercury and plants in contaminated soils: 1. Uptake, partitioning, and emission to the atmosphere. *Environ. Toxicol. Chem.* **1998**, *17* (10), 2063−2071.
(205) Lindberg, S. E.; Price, J. L. Airborne emissions of mercury from municipal landfill operations: a short-term measurement study in Florida. *J. Air Waste Manage. Assoc.* **1999**, *49* (5), 520−532.
(206) Lindberg, S. E.; Turner, R. R. Mercury emissions from chlorine-production solid waste deposits. *Nature* **1977**, *268* (5616), 133−136.
(207) Nguyen, H. T.; Kim, K.-H.; Kim, M.-Y.; Shon, Z.-H. Exchange pattern of gaseous elemental mercury in an active urban landfill facility. *Chemosphere* **2008**, *70* (5), 821−832.
(208) Rinklebe, J.; During, A.; Overesch, M.; Wennrich, R.; Stärk, H.-J.; Mothes, S.; Neue, H.-U. Optimization of a simple field method to determine mercury volatilization from soils - Examples of 13 sites in floodplain ecosystems at the Elbe River (Germany). *Ecol. Eng.* **2009**, *35* (2), 319−328.
(209) Wallschläger, D.; Kock, H. H.; Schroeder, W. H.; Lindberg, S. E.; Ebinghaus, R.; Wilken, R.-D. Estimating gaseous mercury emissions from contaminated floodplain soils to the atmosphere with simple field measurement techniques. *Water, Air, Soil Pollut.* **2002**, *135* (1−4), 39−54.
(210) Wang, S.; Feng, X.; Qiu, G.; Shang, L.; Li, P.; Wei, Z. Mercury concentrations and air/soil fluxes in Wuchuan mercury mining district, Guizhou province, China. *Atmos. Environ.* **2007**, *41* (28), 5984−5993.
(211) Engle, M. A.; Gustin, M. S. Scaling of atmospheric mercury emissions from three naturally enriched areas: Flowery Peak, Nevada; Peavine Peak, Nevada; and Long Valley Caldera, California. *Sci. Total Environ.* **2002**, *290* (1−3), 91−104.
(212) Gustin, S. M.; Coolbaugh, M.; Engle, M.; Fitzgerald, B.; Keislar, R.; Lindberg, S.; Nacht, D.; Quashnick, J.; Rytuba, J.; Sladek, C.; et al. Atmospheric mercury emissions from mine wastes and surrounding geologically enriched terrains. *Environ. Geol.* **2003**, *43* (3), 339−351.
(213) García-Sánchez, A.; Contreras, F.; Adams, M.; Santos, F. Atmospheric mercury emissions from polluted gold mining areas (Venezuela). *Environ. Geochem. Health* **2006**, *28* (6), 529−540.
(214) Gustin, M. S.; Biester, H.; Kim, C. S. Investigation of the light-enhanced emission of mercury from naturally enriched substrates. *Atmos. Environ.* **2002**, *36* (20), 3241−3254.
(215) He, J.; Tan, H.; Sommar, J.; Xiao, Z.; Lindqvist, O. Mercury pollution in a mining area of Guizhou, China: fluxes over contaminated surfaces and concentrations in air, biological and geological samples. *Toxicol. Environ. Chem.* **1998**, *67* (1−2), 225−236.

DOI: 10.1021/acs.est.5b04013
Environ. Sci. Technol. 2016, 50, 507−524